Chapter One
Introduction

1.1 Introduction

Sickle cell disease (SCD) is among the most common of inherited hemoglobinopathies. The disease has been known since James Herrick, a Chicago cardiologist, first reported it as "peculiar elongated and sickle-shaped red corpuscles in a case of severe anemia" (Herrick, 2001). SCD is a multisystem disorder affecting almost every tissue of the body, however it could induces renal dysfunction and further leading to sickle nephropathy in the later stages. Sickle cell nephropathy is indicated by sickled erythrocytes, with the consequent effects of decreased medullary blood flow ischemia, micro-infarct and papillary necrosis (Pham et al, 2000). Clinical features of the disease result from vaso-occlusive consequences of sickled cells more than from the anemia itself. Considering the high prevalence of the disease in certain populations, it is required that reno-vascular changes are detected at an early stage before irreversible organ damage occurs due to chronic vasculopathy. Irreversible organ damage occurs in at least a third of patients, and thus is the most frequent cause of death beyond early childhood (Powars et al, 1990), (Kishor et al, 2008). SCD may result in both renal function disturbances and anatomic alterations. On gray scale sonography evaluation of renal morphologic features in SCD, almost half of the patients with SCD have large kidneys, believed to be a result of increased renal blood volume from the anemia (Walker et al, 1996). Also, the kidneys may display normal echogenicity (89% of patients); may be diffusely, mildly echogenic (5%); or may exhibit increased medullary echogenicity with normal cortical echogenicity (3%). Over time, the kidneys may shrink if renal failure ensues (Harrow et al, 1963). However, most of the gray-scale sonography

morphologic features are observed in the late course of the disease (Kishor et al, 2008).

Previous literature describes the application of renal sonography in the assessment of renal dysfunction in many diseases including renal artery stenosis (Avasthi et al, 1984) acutely obstructed kidneys (Rodgers et al, 1992). And acute renal failure in determining grafts survival in transplanted kidneys and in SCD (Aikimbaev et al, 1996), (Guvenc et al, 2005). However, the trend of this study is focusing on the impacts of SCD in kidneys *(Morphology & Physiology)* and to reveal how far renal ultrasonography (*grayscale & doppler*) would be applicable and utilizable in early diagnosis/predictors of renal pathology among patients with SCD.

1.2 Problem of the study

Sickle-cell anemia is one of the most common diseases encountering the anatomical and physiological characteristics of kidneys.

Delay of diagnosis might lead to severe complications resulting in progressive damage to most organs, including the kidneys, liver, lungs, brain, bones, and cardiovascular system, which becomes apparent with increasing age.

Renal sonography can serve as early ultrasonic predictors of reno-vascular changes in sickle cell anemia. Thereby these findings can guide clinicians to initiate adequate treatment at an early stage.

1.3 Objectives

The general objective of this study was to evaluate the impact of sickle cell disease (SCD) in kidneys morphology and physiology by using ultrasonography in Sudan.

Specific objectives:

- To measure the size of SCD patient's kidneys relative to control group.
- To assess the SCD impact on echogenicity of kidneys.
- To measure resistive and pulsatilty indices of renal arteries for SCD patients.
- To find correlation of age to RI & PI of renal arteries among SCD patients relative to control group.
- To correlate BMI with RI & PI of renal arteries among SCD patients relative to control group.

1.4 Significance of the study

This study will highlight the significance of U/S to be utilized as an early diagnosis and predictor for the complications of SCD impact in kidneys in Sudanese population.

1.5 Overview of the study

This study will falls into five chapters, chapter one is an introduction which is include the problem of the study, objective, significance of the study and overview. While chapter two contain scholar literature about the problem of the study as well chapter three include the material used to collect the data and method of data collection. Chapter four include result presentation using tables and figure and finally chapter five will present discussion of the presented result as well as conclusion and recommendation.

Chapter Two
Literature review

2.1 Anatomy of the kidney

The paired kidneys are reddish, kidney bean–shaped organs located just above the waist between the peritoneum and the posterior wall of the abdomen. Because their position is posterior to the peritoneum of the abdominal cavity, they are said to be retroperitoneal organs (Figure 2.1). The kidneys are located between the levels of the last thoracic and third lumbar vertebrae, a position where they are partially protected by the eleventh and twelfth pairs of ribs. Unfortunately, if these lower ribs are fractured, they can puncture the kidneys and cause significant and even life-threatening, damage. The right kidney is slightly lower than the left (Figure 2.2) because the liver occupies considerable space on the right side superior to the kidney (Gerard & Bryan, 2012).

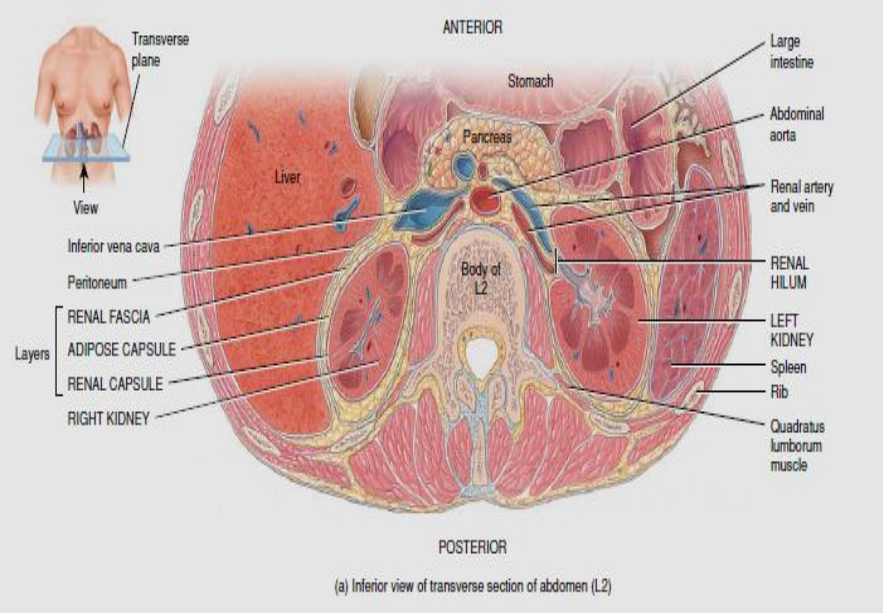

Figure 2.1.*Position and coverings of the kidneys (Gerard & Bryan, 2012).*

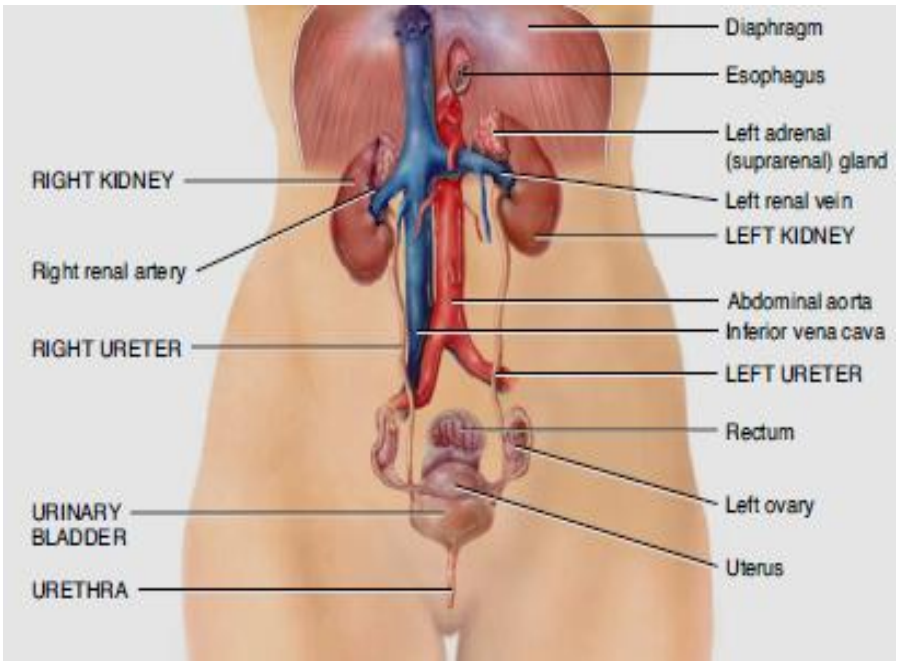

Figure 2.2.*Organs of the urinary system in a female (Gerard & Bryan, 2012).*

2.1.1External Anatomy of the Kidneys

A typical adult kidney is 10-12 cm long, 5-7 cm width, and 3 cm thickness-about the size of a bar of bath soap—and has a mass of 135-150g. The concave medial border of each kidney faces the vertebral column (Figure 2.1). Near the center of the concave border is an indentation called the renal hilum or hilus (Figure 2.3), through which the ureter emerges from the kidney along with blood vessels, lymphatic vessels and nerves (Gerard & Bryan, 2012).

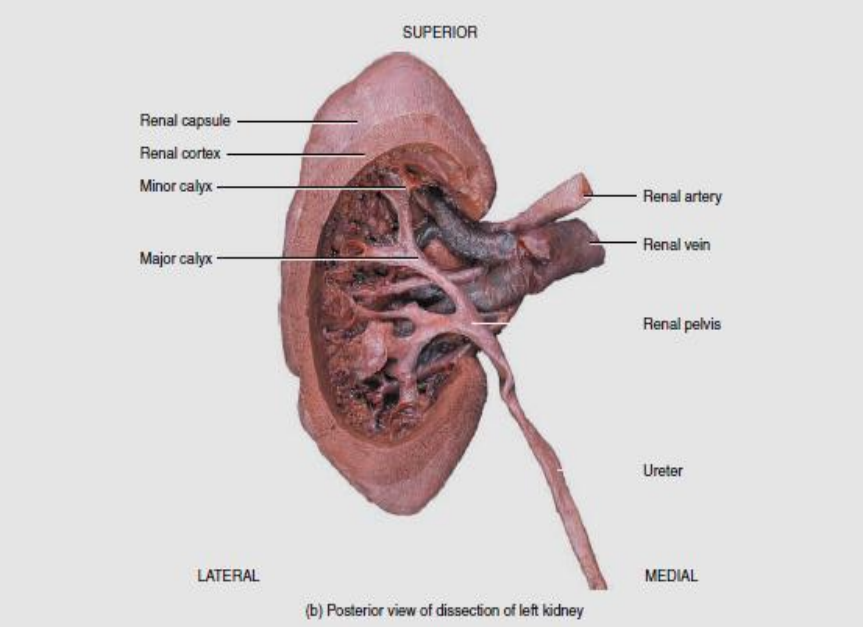

Figure 2.3.*Internal anatomy of the kidneys (Gerard & Bryan, 2012).*

Three layers of tissue surround each kidney (Figure 2.4). The deep layer, the renal capsule, is a smooth, transparent sheet of dense irregular connective tissue that is continuous with the outer coat of the ureter. It serves as a barrier against trauma and helps maintain the shape of the kidney. The middle layer, the adipose capsule, is a mass of fatty tissue surrounding the renal capsule. It also protects the kidney from trauma and holds it firmly in place within the abdominal cavity. The superficial layer, the renal fascia, is another thin layer of dense irregular connective tissue that anchors the kidney to the surrounding structures and to the abdominal wall. On the anterior surface of the kidneys, the renal fascia is deep to the peritoneum (Gerard & Bryan, 2012).

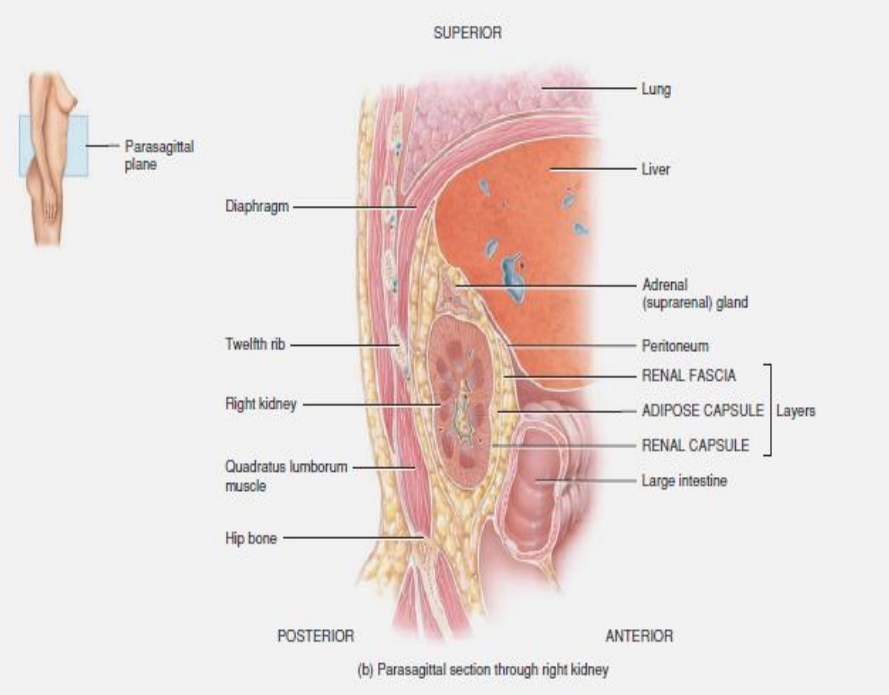

Figure 2.4.*Position and coverings of the kidneys (Gerard & Bryan, 2012).*

2.1.2 Internal Anatomy of the Kidneys

A frontal section through the kidney reveals two distinct regions: a superficial, light red area called the renal cortex (*cortex* -rindor bark) and a deep, darker reddish-brown inner region called the renal medulla (*medulla* - inner portion) (Figure 2.5). The renal medulla consists of several cone-shaped renal pyramids**.** The base (wider end) of each pyramid faces the renal cortex, and its apex (narrower end), called a renal papilla**,** points toward the renal hilum. The renal cortex is the smooth-textured area extending from the renal capsule to the bases of the renal pyramids and into the spaces between them. It is divided into an outer *cortical zone* and an inner *juxta-medullary zone*.

Those portions of the renal cortex that extend between renal pyramids are called renal columns. A renal lobe consists of a renal pyramid, its overlying area of renal cortex, and one-half of each adjacent renal column (Gerard & Bryan, 2012).

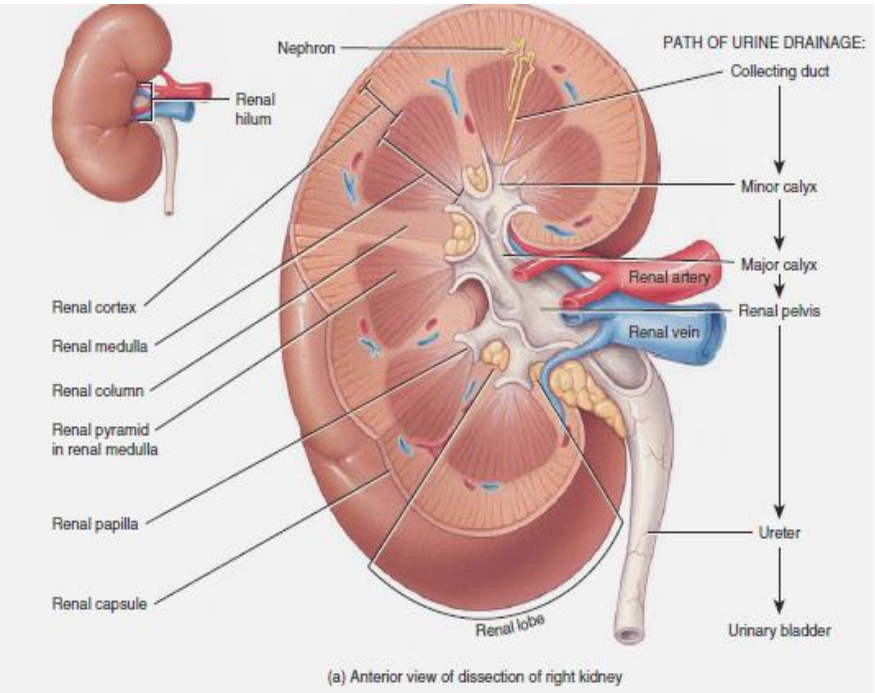

Figure 2.5.*Position and coverings of the kidneys (Gerard & Bryan, 2012).*

Together, the renal cortex and renal pyramids of the renal medulla constitute the parenchyma or functional portion of the kidney. Within the parenchyma are the functional units of the kidney-about 1 million microscopic structures called nephrons. Filtrate (filtered fluid) formed by the nephrons drains into large papillary ducts**,** which extend through the renal papillae of the pyramids. The papillary ducts drain into cuplike structures called minor and major calyces. Each kidney has 8 to 18 minor calyces and 2 or 3 major calyces. A minor calyx receives urine from the papillary ducts of one renal papilla and delivers it to a major calyx. Once the filtrate enters the calyces it becomes urine because no further re-absorption can occur. The reason for this is that the simple epithelium of the nephron and ducts becomes transitional epithelium in the calyces. From the major calyces, urine drains into a single large cavity called the renal pelvis and then out through the ureter to the urinary bladder (Tortora & Derrickson, 2012).

The hilum expands into a cavity within the kidney called the renal sinus**,** which contains part of the renal pelvis, the calyces, and branches of the renal blood vessels and nerves. Adipose tissue helps stabilize the position of these structures in the renal sinus (Tortora & Derrickson, 2012).

2.1.3 Blood and Nerve Supply of the Kidneys

Because the kidneys remove wastes from the blood and regulate its volume and ionic composition, it is not surprising that they are abundantly supplied with blood vessels. Although the kidneys constitute less than 0.5% of total body mass, they receive 20-25%of the resting cardiac output via the right and left renal arteries (Figure 2.6). In adults, renal blood flow, the blood flow through both kidneys, is about 1200 mL per minute (Tortora & Derrickson, 2012).

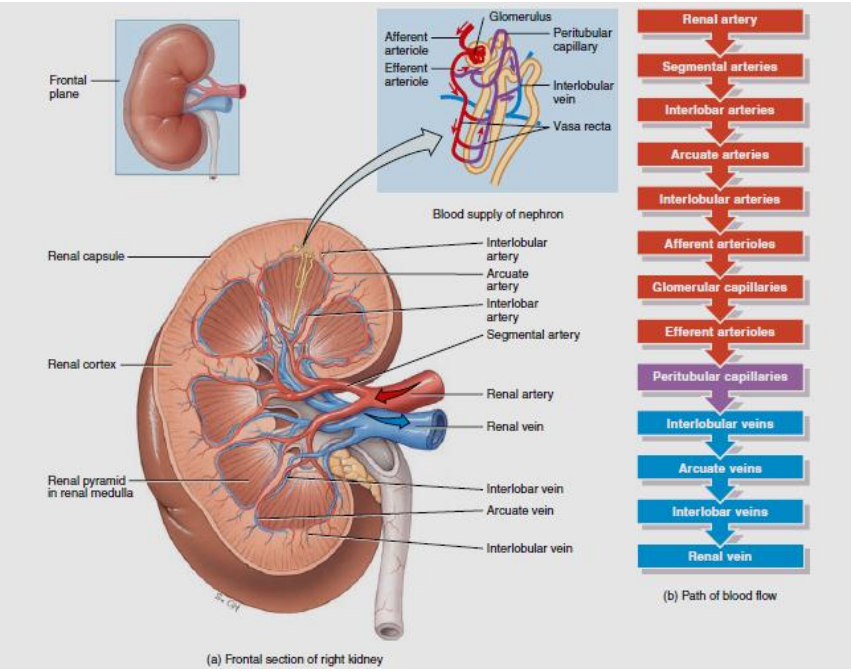

Figure 2.6.*Blood supply of the kidney (Gerard & Bryan, 2012).*

Within the kidney, the renal artery divides into several segmental arteries, which supply different segments (areas) of the kidney. Each segmental artery gives off several branches that enter the parenchyma and pass through the renal columns between the renal pyramids as the inter-lobar arteries. At the bases of the renal pyramids, the inter-lobar arteries arch between the renal medulla and cortex; here they are known as the arcuate arteries (Tortora & Derrickson, 2012).

Divisions of the arcuate arteries produce a series of inter-lobular arteries. These arteries are so named because they pass between renal lobules. Interlobular arteries enter the renal cortex and give off branches called afferent arterioles. Each nephron receives one afferent arteriole, which divides in to a tangled, ball-shaped capillary network called the glomerulus. The glomerular capillaries then reunite to form an efferent arteriole that carries blood out of the glomerulus. Glomerular capillaries are unique among capillaries in the body because they are positioned between two arterioles, rather than between an arteriole and a venule. Because they are capillary networks and they also play an important role in urine formation, the glomeruli are considered part of both the cardiovascular and the urinary systems (Tortora & Derrickson, 2012).

The efferent arterioles divide to form the peritubular capillaries, which surround tubular parts of the nephron in the renal cortex. Extending from some efferent arterioles are long loop-shaped capillaries called vasa recta that supply tubular portions of the nephron in the renal medulla (Figure 2.7).

The peritubular capillaries eventually reunite to form peritubular venules and then interlobular veins, which also receive blood from the vasa recta. Then the blood drains through the arcuate veins to the inter-lobar veins running between the renal pyramids. Blood leaves the kidney through a single renal vein that exits at the renal hilum and carries venous blood to the inferior vena cava.

Many renal nerves originate in the renal ganglion and pass through the renal plexus into the kidneys along with the renal arteries. Renal nerves are part of the sympathetic division of the autonomic nervous system. Most are vasomotor nerves that regulate the flow of blood through the kidney by causing vasodilation or vasoconstriction of renal arterioles (Tortora & Derrickson, 2012).

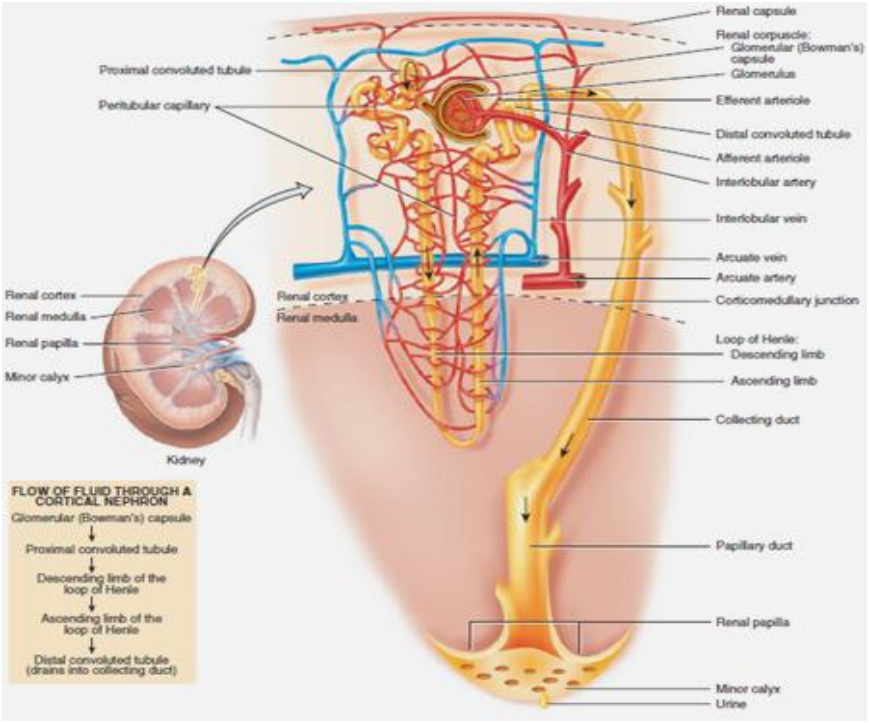

Figure 2.7.*The structure of nephrons and & blood vessels (Tortora & Derrickson, 2012).*

2.2 Physiology of the kidney

The kidneys do the major work of the urinary system. The other parts of the system are mainly passageways and storage areas. Functions of the kidneys include the following:

2.2.1 Regulation of blood ionic composition. The kidneys help regulate the blood levels of several ions, most importantly sodium ions, potassium ions, calcium ions, chloride ions, and phosphate ions.

2.2.2 Regulation of blood pH. The kidneys excrete a variable amount of hydrogen ions into the urine and conserve bicarbonate ions, which are an important buffer of hydrogen in the blood. Both of these activities help regulate blood pH.

2.2.3 Regulation of blood volume. The kidneys adjust blood volume by conserving or eliminating water in the urine. An increase in blood volume increases blood pressure; a decrease in blood volume decreases blood pressure.

2.2.4 Regulation of blood pressure. The kidneys also help regulate blood pressure by secreting the enzyme renin, which activates the rennin-angiotensin-aldosterone pathway (Figure 2.8). Increased renin causes an increase in blood pressure.

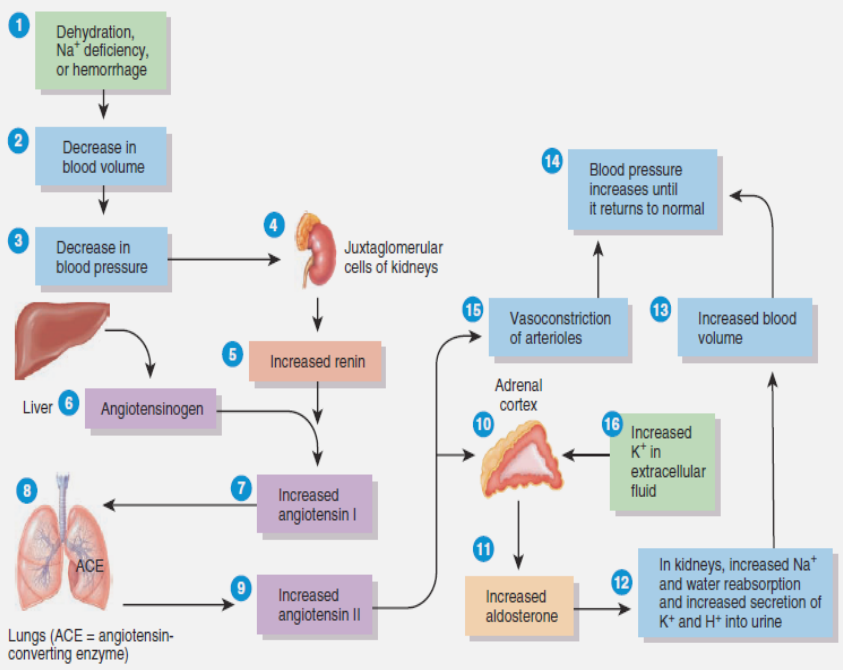

Figure 2.8.*Regulation of aldosterone secretion by the renin–angiotensin–aldosterone (RAA) pathway (Tortora & Derrickson, 2012).*

2.2.5 Maintenance of blood osmolarity. By separately regulating loss of water and loss of solutes in the urine, the kidneys maintain a relatively constant blood osmolarity close to 300 milliosmoles per liter (mOsm/liter).

2.2.6 Production of hormones. The kidneys produce two hormones.

-*Calcitriol*, the active form of vitamin D, helps regulate calcium homeostasis (Figure 2.9).

-*Erythropoietin* stimulates the production of red blood cells (Figure 2.10).

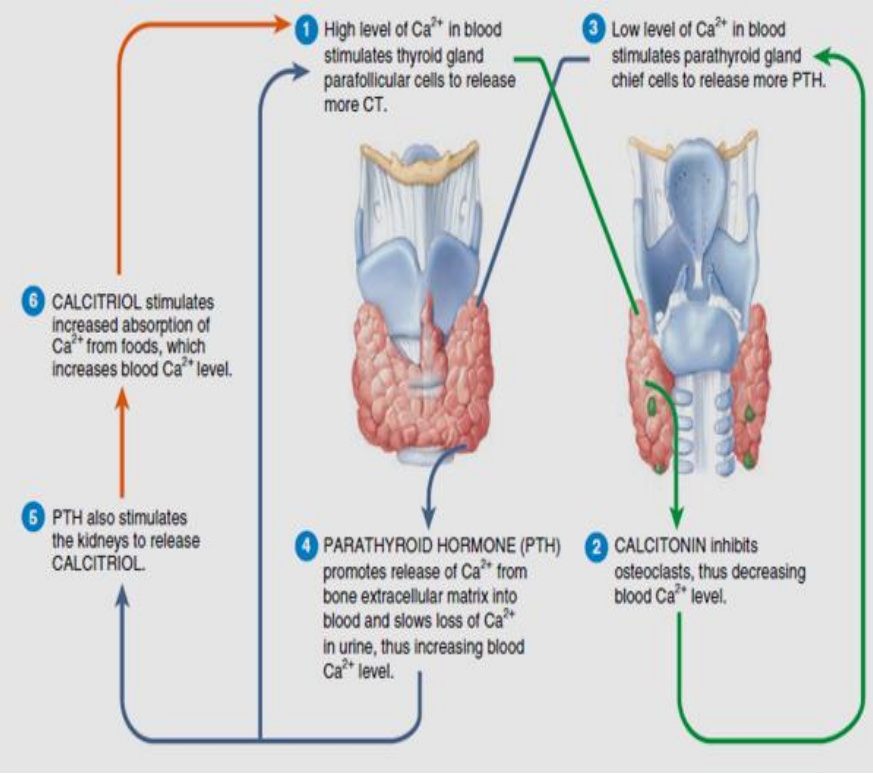

Figure 2.9.*The roles of calcitonin (green arrows), parathyroid hormone (blue arrows), and calcitriol (orange arrows) in calcium homeostasis (Tortora & Derrickson, 2012).*

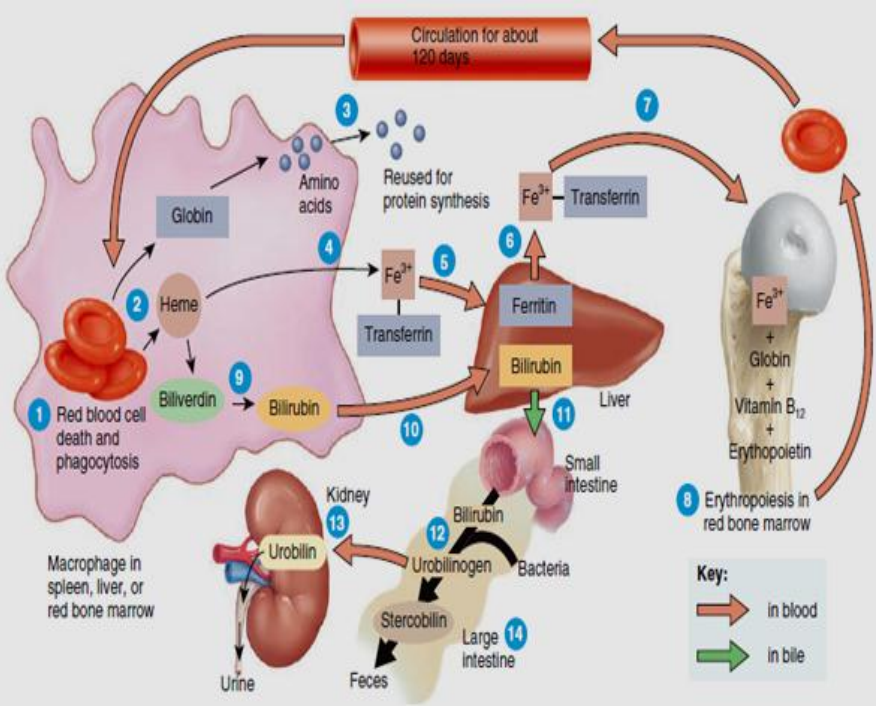

Figure 2.10.*Formation and destruction of red blood cells, and the recycling of hemoglobin components (Tortora & Derrickson, 2012).*

2.2.7 Regulation of blood glucose level. Like the liver, the kidneys can use the amino acid glutamine in *gluconeogenesis,* the synthesis of new glucose molecules. They can then release glucose into the blood to help maintain a normal blood glucose level.

2.2.8 Excretion of wastes and foreign substances. By forming urine, the kidneys help excrete wastes-substances that have no useful function in the body. Some wastes excreted in urine result from metabolic reactions in the body. These include ammonia and urea from the deamination of amino acids; bilirubin from the catabolism of hemoglobin; creatinine from the breakdown of creatine phosphate in muscle fibers; and uric acid from the catabolism of nucleic acids. Other wastes excreted in urine are foreign substances from the diet, such as drugs and environmental toxins (Tortora & Derrickson, 2012).

Nephrons are the functional units of the kidneys. Each nephron (Figure 2.7) consists of two parts: a renal corpuscle, where blood plasma is filtered, and a renal tubule into which the filtered fluid passes. The two components of a renal corpuscle are the glomerulus (capillary network) and the glomerular (Bowman's) capsule, a double-walled epithelial cup that surrounds the glomerular capillaries. Blood plasma is filtered in the glomerular capsule, and then the filtered fluid passes into the renal tubule, which has three main sections. In the order that fluid passes through them, the renal tubule consists of; Proximal convoluted tubule or PCT, Loop of Henle and distal convoluted tubule or DCT. Pr*oximal* denotes the part of the tubule attached to the glomerular capsule, and *distal* denotes the part that is further away. *Convoluted* means the tubule is tightly coiled rather than straight (Tortora & Derrickson, 2012).

The renal corpuscle and both convoluted tubules lie within the renal cortex; the loop of Henle extends into the renal medulla, makes a hairpin turn, and then returns to the renal cortex. The distal convoluted tubules of several nephrons empty into a single collecting duct**,** Collecting ducts then unite and converge into several hundred large papillary ducts, which drain into the minor calyces. The collecting ducts and papillary ducts extend from the renal cortex through the renal medulla to the renal pelvis, so one kidney has about 1 million nephrons, but a much smaller number of collecting ducts and even fewer papillary ducts. In a nephron, the loop of Henle connects the proximal and distal convoluted tubules. The first part of the loop of Henle dips into the renal medulla, where it is called the descending limb of the loop of Henle (Figure 2.7). It then makes that hairpin turn and returns to the renal cortex as the ascending limb of the loop of Henle. About 80-85% of the nephrons are cortical nephrons. Their renal corpuscles lie in the outer portion of the renal cortex, and they have short loops

of Henle that lie mainly in the cortex and penetrate only into the outer region of the renal medulla (Figure 2.7) (Tortora & Derrickson, 2012).

The short loops of Henle receive their blood supply from peritubular capillaries that arise from efferent arterioles. The other 15-20% of the nephrons are juxtamedullary nephrons. Their renal corpuscles lie deep in the cortex, close to the medulla, and they have a *long* loop of Henle that extends into the deepest region of the medulla (Figure 2.7). Long loops of Henle receive their blood supply from peritubular capillaries and from the vasa recta that arise from efferent arterioles. In addition, the ascending limb of the loop of Henle of juxtamedullary nephrons consists of two portions: a thin ascending limb followed by a thick ascending limb (Figure 2.7). The lumen of the thin ascending limb is the same as in other areas of the renal tubule; it is only the epithelium that is thinner. Nephrons with long loops of Henle enable the kidneys to excrete very dilute or very concentrated urine (Tortora & Derrickson, 2012).

2.3 Pathology of the kidney

2.3.1 Congenital cystic kidneys

This occurs in two main forms, one of which does not usually cause illness until beyond the age of 30 years while the other is usually fatal in infancy.

Adult polycystic disease; Polycystic kidney disease (PKD) encompasses a group of inherited disorders that result in cyst development in the kidney in addition to a range of extra-renal manifestations (Torres, 2007). Autosomal dominant PKD (ADPKD) and autosomal recessive PKD (ARPKD) are common, simple forms of PKD, in which renal and liver disease account for most of the morbidity. Additionally, a number of syndromic diseases, such as Meckel (MKS), Joubert (JBTS) and Bardet Biedl (BBS) syndromes, have PKD as a major phenotypic manifestation (Hildebrandt, et al. 2011). ARPKD has a frequency of

approximately 1:20,000, and the typical presentation is of severe PKD detected in utero or in the perinatal period with greatly enlarged kidneys, which is associated with significant neonatal mortality (Sweeney & Avner. 2014). However, ARPKD may first present later in childhood or even in adulthood with less evident renal enlargement and complications of congenital hepatic fibrosis as the major cause of symptomatic disease (Adeva, et al. 2006).

Infantile polycystic disease is rare and usually leads to renal failure in infancy or early childhood. It may be due to an autosomal recessive trait. The kidneys contain multiple elongated radially arranged cysts lined by cuboidal or columnar epithelium. Renal enlargement may be sufficient to interfere with birth or, in live born infants, with respiration (Adeva, et al. 2006).

Medullary sponge kidney shows cystic dilatation of the collecting ducts in the papillae. It is usually bilateral and may affect any or all of the papillae in each kidney. Symptoms usually develop after the age of 30, and are due to the formation of calculi within the cysts or to superadded pyelonephritis. The cysts are usually less than 5mm in diameter and their epithelial lining may be single-layered, squamous or transitional. The diagnosis may be apparent from intravenous pyelograms. Its cause is unknown (Adeva, et al. 2006).

Simple renal cysts (Figure 2.11) very common and most individuals over the age of 45 have one or more. Occasionally multiple, they show an increasing incidence with age and also in kidneys damaged by pyelonephritis and glomerulo-nephritis and in end-stage kidneys in patients on chronic dialysis. Such cysts are obviously secondary in nature (Deam, et al. 2002).

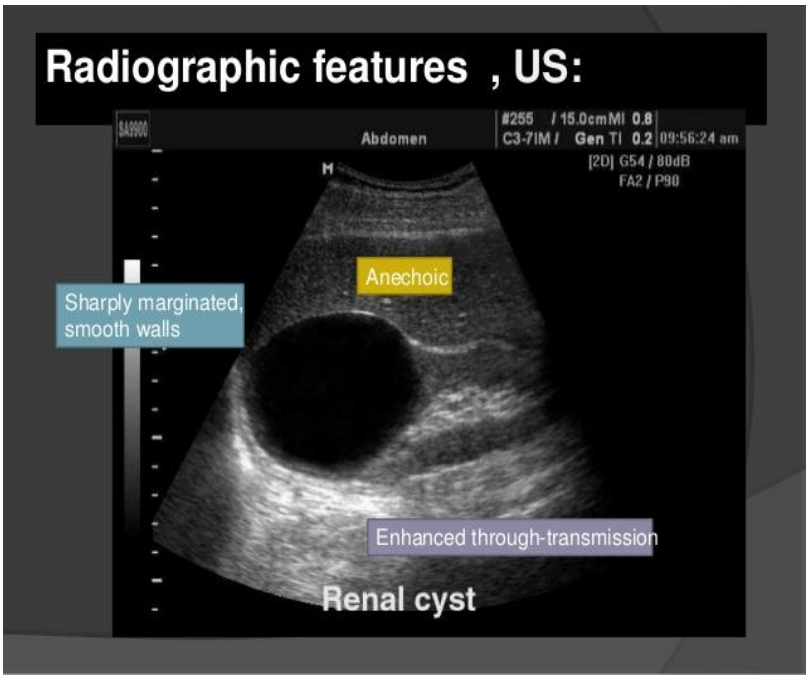

Figure 2.11.*Simple renal cyst (www.google scholar.com).*

2.3.2 Other congenital renal defects

These are numerous and some are comparatively common. Occasionally one kidney, usually the left, is absent-agenesis-and in these cases the ureter is also absent, as a result, the surviving kidney undergoes compensatory hypertrophy. This occurs also in hypoplasia of one kidney, which appears usually as an irregular atrophic structure around the upper end of its ureter. If bilateral, hypoplasia will result in renal failure.

Sometimes, the kidneys are fused, most often at the lower pole - '*horseshoe kidney*': the two ureters pass in front of the connecting bridge. One kidney, more rarely both, may lie in an ectopic position in front of the sacrum. The kidney is originally composed of five lobules and ordinary their fusion is complete. If incomplete the term *fetal lobulation* is applied: the condition is of no importance. The arrangement of the renal arteries is very variable and there may be one, two or occasionally multiple arteries (Deam, et al. 2002).

2.3.3 Urinary tract infection and pyelonephritis

Urinary tract infection involves either the bladder (cystitis) or the kidneys and the renal pelvis (pyelonephritis) or both. The single most important criterion of urinary tract infection is the presence of bacteria in the urine. In urine obtained through a bladder catheter the presence of any organisms is significant, while in the commonly used mid strem sample there is bound to be some contamination by urethral or perirenal organisms. Thus, in such samples a bacterial count of more than 1000000 per ml is the accepted definition of infection. Bacteriuria in the absence of symptoms is termed asymptomatic or covert bacteriuria and it is of importance under two circumstances: first, in infancy, if associated with ureteric reflux, it can lead to ascent of infection to the kidneys; second in pregnancy, where it might be followed by symptomatic infection and can predispose to pre-eclampsia and prematurity (Deam, et al. 2002).

Urinary tract infection occurring without preceding catheterization or obstruction is usually due to bacteria normally present in the faeces, in most cases *Escherichia coli*, but sometimes *Klebsiella*, *Proteus* spp. or *Pseudomonas* spp. are responsible. Infection complicating obstruction or instrumentation is commonly of mixed bacterial type, *E. coli*. *Proteus* spp. and staphylococci being most often present. Hematogenous spread may also occur but is much less common; it may arise in the course of acute pyemia or septicemia complicating staphylococcal infections or infective endocarditis.

By far the commonest route of infection is along the lumen of the urethra. The incidence of infection is higher in females throughout all age ranges with a sex ratio of 20:1 in children and young adults but this sex ratio falls in old age due to the increasing incidence of prostatic hypertrophy. The female preponderance is due mainly to the ease with which endogenous infections can ascend the short

female urethra. Precipitating factors include trauma to the perineum during sexual intercourse or childbirth (Deam, et al. 2002).

Most urinary infections in females occur in anatomically normal urinary tracts and the vast majority of these are confined to the bladder. In a small percentage of females and relatively more often in males, stagnation of urine resulting from urinary tract obstruction is the main etiological factor. Causes include urethral obstruction by inflammatory scarring or congenital, valve-like mucosal folds, urinary calculi, diverticula and tumours of the bladder, congenital malformations such as double ureters, and neurological disorders, e.g. paraplegia or multiple sclerosis which interfere with emptying of the bladder. In men, prostatic enlargement is the commonest predisposing cause of urinary tract infection.

When confined to the bladder, urinary infection is termed cystitis and is characterized by dysuria, increased frequency of micturition and sometimes hematuria. The ascent of infection to the kidneys is usually due to vesicoureteric reflux, urinary tract obstruction or pregnancy (Deam, et al. 2002).

Pyelonephritis is a bacteria-induced inflammation of the renal pelvis, calyces and renal parenchyma. It can occur in acute and chronic forms and can affect one or both kidneys. The vast majority of cases are due to ascending infection, often in association with vesicoureteric reflux, while in a very small proportion organisms reach the kidney through the bloodstream. The predominant organisms responsible for ascending infection are faecal flora as has already been mentioned, but virtually any bacteria or fungus can cause renal infection.

Tuberculosis*:* This is becoming increasingly uncommon. The bladder may be affected as a result of direct mucosal infection most often in cases of renal tuberculosis but sometimes in tuberculosis of the genital tract. Tuberculous pyelonephritis results from blood spread, usually from pulmonary lesions. Minute tubercles are seen in acute miliary tuberculosis. Localized lesions of

tuberculous pyelonephritis may slowly extend to destroy the kidneys. The disease can also involve the ureters, bladder and other pelvic viscera. Renal pelvic involvement often results in hematuria and the renal lesions tend also to suppurate, giving pyuria (Deam, et al. 2002).

2.3.4 Glomerulonephritis

This term embraces a group of renal diseases in which the lesions are primarily glomerular. Although the name implies inflammation, the typical histological features of inflammation are not present in all types. Glomerulonephritis can be classified on either a clinical or pathological basis but the latter is preferable in view of its greater precision and better correlation with pathogenetic mechanisms. Response to therapy and prognosis, Also some forms of glomerulonephritis consist of diseases confined to the kidneys, such as diffuse membranous glomerulonephritis, while with others the disease may be systemic, e.g. Systemic lupus erythomatosus (SLE) (Deam, et al. 2002).

2.3.5 Vascular disease of the kidney

The renal vessels show the usual features of generalized vascular diseases. Atheroma occurs but is much less common than in other arteries of comparable size and except in patients with diabetes mellitus, it is rarely severe enough to interfere with the renal circulation. Disturbances arise more commonly from involvement and narrowing at the origin of one or rarely both renal arteries by atheromatous plaques. Unilateral renal artery stenosis accounts for less than 5% of cases of hypertension. In addition to atheroma, renal artery stenosis may be the result of fibromuscular dysplasia and this account for about a third of cases. Hypertension results from the renal ischemia. It is important to make the diagnosis of unilateral renal artery stenosis as surgical treatment may cure the hypertension (Deam, et al. 2002).

2.3.6 Renal changes in hypertension

The arterial tree of the kidney usually affected more than other organs and this results in varying degrees of renal damage. In benign (essential) hypertension the renal injury is usually slight and there is often minimal functional impairment, whereas is malignant (accelerated) hypertension severe arteriolar damage in the form of arteriolar necrosis gives rise to renal failure.

Benign hypertension; Hypertensive arteriosclerosis of the larger branches of the renal arteries is without any functional effects; the interlobular arteries may be narrowed in severe arteriosclerosis by the fibroelastic intimal thickening, but the most significant lesion, hyaline arteriosclerosis, occur mainly in the afferent glomerular arterioles which become tortuous, thick-walled and often severely narrowed. These arterial changes tend to cause ischemia and individual nephrons are affected. The capillary tuft of the affected glomerulus shrinks, and becomes hylainized, and *Bowman's* capsule becomes filled with collagen. The tubules atrophy and are replaced by fibrous tissue often containing some lymphocytes.

In the early stages of hypertension the kidney appears normal, but with prominent arteries visible on the cut surface. As more nephrons are lost there is diffuse thinning of the renal cortex and kidneys become moderately reduced in size, with an average weight of about 115g. If enough nephrons are lost there may be hypertrophy of the surviving nephrons. The kidneys are seldom very small and while there may be loss of functional reserve, renal function is not significantly impaired (Deam, et al. 2002).

Malignant hypertension*;* this may be arise acutely, apparently *de novo*, or may supervene after a variable period of benign hypertension, and the appearances in the kidney vary accordingly. In the most acute cases the surface of the kidney is smooth and spotted with tiny petechial hemorrhages. The cut surface may show mottling due to multiple tiny infarcts. The interlobular arteries may show intimal

thickening. Fibrinoid necrosis affects mainly the distal portions of the interlobular arteries and the afferent arterioles and may extend into the glomerular tuft. There is often blood or proteinaceous fluid in Bowman's space and sometimes proliferation of the capsular epithelium may give rise to small crescents. A minority of the glomeruli are affected, the severe impairment of renal function being due to ischemia caused by the severe arterial damage. The tubules may be atrophied or enlarged and usually contain proteinaceous or blood casts (Deam, et al. 2002).

There is hyperplasia of the rennin-secreting cells of the juxtaglomerular apparatus, correlating with the high serum levels of rennin and angiotensin II in malignant hypertension. In contrast to benign hypertension, renal failure is common in untreated cases.

Secondary hypertension; various grades of hypertension may complicate pre-existing renal diseases. Depending on the height and rate of rise of the blood pressure, the renal changes of benign and/or malignant hypertension may be superimposed on those of the primary renal disease (Deam, et al. 2002).

2.3.7 Urinary tract obstruction

Obstruction in the urinary tract may be of sudden or insidious onset, may be intermittent or complete, may bilateral or unilateral and may predispose to urinary tract infection and calculus formation.

Serious mechanical obstruction of the urethra is practically confined to the male sex. Neurogenic disturbance of the bladder occurs in spina bifida and following trauma or pressure on the spinal cord. In addition to pressure effects, in pregnancy the effect of high progesterone levels in relaxing smooth muscle may result in functional dilatation of ureters and pelvis with so-called dysfunctional obstruction. In many instances of unilateral hydronephrosis severe narrowing of the ureter occurs at the pelviureteric junction, but without scarring: it may

represent a congenital structural abnormality or result from some form of neuromuscular dysfunction. Kinking of the ureter by an aberrant renal artery to the lower pole of the kidney may also cause hydronephrosis (Deam, et al. 2002).

In urethral obstruction, the chief effect is the production of variable degrees of hypertrophy and dilatation of the bladder wall. When the outstanding feature is hypertrophy, the muscular part of the wall is thickened and the bands of muscle, which have an interlacing arrangement under the mucosa, enlarge and form prominent ridges or bands with depressions between. Occasionally one of these depressions may become enlarged and form a diverticulum in which infection suppuration, ulceration and even perforation may fallow. Urethral obstruction ultimately leads to dilatation of the ureters and renal pelvis-hydroureter and hydronephrosis (Deam, et al. 2002).

2.3.8 Hydronephrosis

Hydronephrosis (Figure 2.12, a & b) is a dilatation of the renal pelvis and calyces due to obstruction of urinary outflow; this can lead to progressive renal atrophy with fibrosis because the pressure in the renal pelvis is transferred back to the collecting tubule and the nephron. Glomerular filtration persists for some time, even with complete obstruction, and so the affected calyces and pelvis may become markedly dilated. Tubular function is affected by the increasing pressure with impaired ability to concentrate the urine (Deam, et al. 2002).

As the distension progresses the calyces become flattened; the renal parenchyma becomes progressively thinned and may ultimately from a mere rind enclosing a cystic structure in which the normal kidney architecture cannot be defined. Atrophy of the renal parenchyma may be regular or irregular so that some areas may be spared while the rest is severely thinned. Histologically, there is tubular atrophy, glomerular fibrosis and a superimposed chronic inflammatory cell infiltrate.

Clinical features. These depend on the site of obstruction and whether it is sudden and/or complete. Acute obstruction may give rise to pain due to rapid distension; ureteric obstruction due to a renal calculus is exquisitely painful; uretheral obstruction due to prostatism will result in bladder distension. Unilateral hydroureter and hydronephrosis may be clinically silent, renal function being maintained by the other kidney. Bilateral complete obstruction will result in rapidly progressive renal failure. Bilateral incomplete obstruction results initially in tubular dysfunction with impairment of urine concentration, producing polyuria and nocturia. Superimposed urinary tract infection will produce additional symptoms, mainly dysuria, fever and loin pain. Renal failure will progress slowly (Deam, et al. 2002).

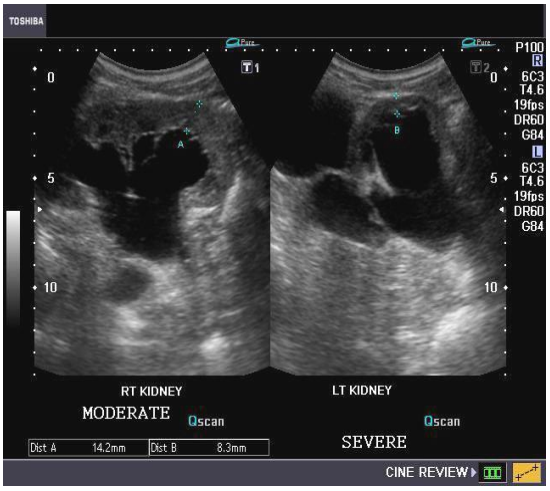

Figure 2.12 (a).*Mild hydronephrosis (Radiopedia).*

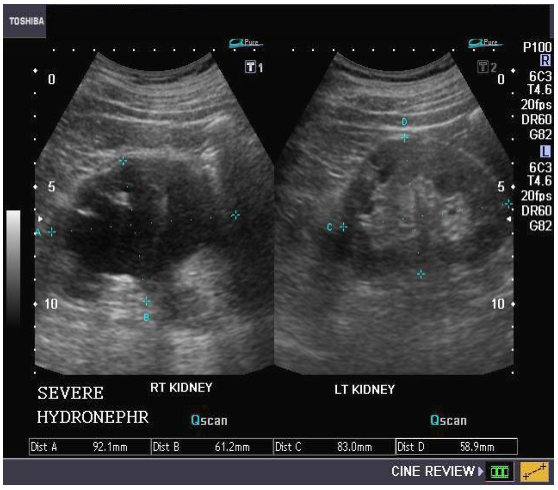

Figure 2.12 (b).*Severe hydronephrosis (Radiopedia).*

2.3.9 Renal calculi

Stones in the renal pelvis may be single or multiple. They are sometimes particularly numerous when there is partial obstruction and dilatation. A single calculus may, however, grow to the size and shape of the dilated pelvis, the so-called stag-horn calculus.

A small calculus may pass down the ureter to the bladder, giving rise to renal colic with hematuria. It may be arrested temporarily, usually at the narrow lower end of the ureter. Permanent impaction, usually at the upper or lower ends of the ureter or at the level of the pelvis brim, produces hydronephrosis. When the urine is infected with urea splitting bacteria (e.g. *Proteus* spp.) ammonia is produced and calculi or softer deposits composed of phosphates form in the alkaline urine and are precipitated in the inflamed pelvis. The condition may be accompanied by suppuration (pyonephrosis) and ulceration. The branching staghorn calculi arise in this way and composed largely of complex hydrated phosphate. A calculus in the renal pelvis, especially when it is movable, may give rise to metaplasia of the lining of the pelvis to stratified squamous epithelium and there is a risk of the development of squamous-cell carcinoma (Deam, et al. 2002).

2.3.10 Renal failure

May develop in both acute and chronic renal failure (Figure 2.13, a & b). In the hepato-renal syndrome there is impairment of renal function without morphological damage. It is characterized by a reduced glomerular filtration rate and progressive oliguria, but without a fall in urine osmolarity. The mechanisms are unknown but the renal failure is reversible with improvement in hepatic function. Acute renal failure may also results from hypotension due to bleeding from esophageal varices or as an additional complication when the liver failure

is of a drug-induced etiology. In these cases the kidneys show the features of acute tubular necrosis (Deam, et al. 2002).

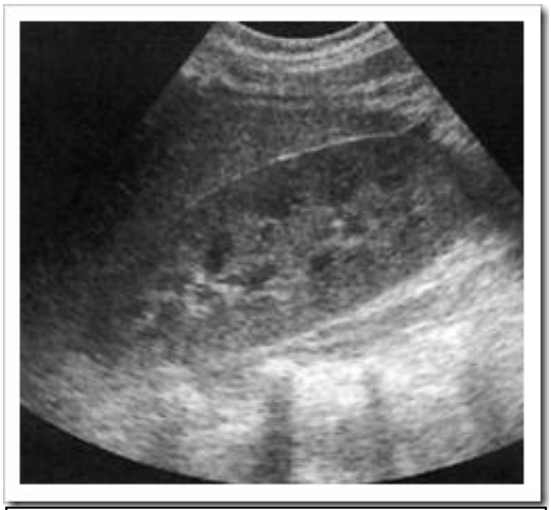

Figure 2.13 (a).*Acute renal failure (Radiopedia).*

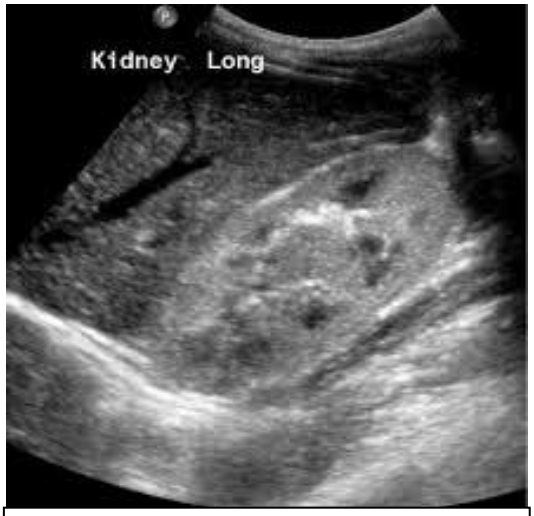

Figure 2.13(b).*Chronic renal failure (Radiopedia).*

2.3.11 Tumors of the kidney

Tumours of the kidney and urinary tract are not uncommon. They tend to bleed and hematuria is the commonest symptom. Infection may also occur and recurrent cystitis is not unusual with ulcerated tumours. Symptoms may also arise from local invasion or distant metastases, sometimes in unusual sites, may occur with renal cell carcinoma (Deam, et al. 2002).

Benign tumors; the commonest benign intra-renal tumour is a small fibroma of the medulla derived from the interstitial cells.

Adenomas; which usually develop in the cortex, are more commonly seen in the end-stage kidneys of patients who are long-term dialysis or who have received a renal transplant. Apart from this they are rare. They are usually benign, but occasionally may metastasize. Histologically, they resemble renal cell adenocarcinomas and because of this the size of an adenoma is arbitrarily used

as a diagnostic criterion: tumours less than 3cm in diameter are usually benign and any larger than this may metastasize (Deam, et al. 2002).

Angiomyolipomas; (Figure 2.14), comprising an admixture of vessels, smooth muscle and adipose tissue, are common in patients with tuberous sclerosis. In the renal pelvis *villous papillary tumours* are sometimes seen; they correspond to the papillary tumours of the bladder and they may be concurrent. *Angiomas* are uncommon, occur in the pyramids or just beneath the lining of the pelvis, but even when small, may lead to severe hematuria. *Rennin-producing tumours* of the juxta-glomerular apparatus occur but are extremely rare (Deam, et al. 2002).

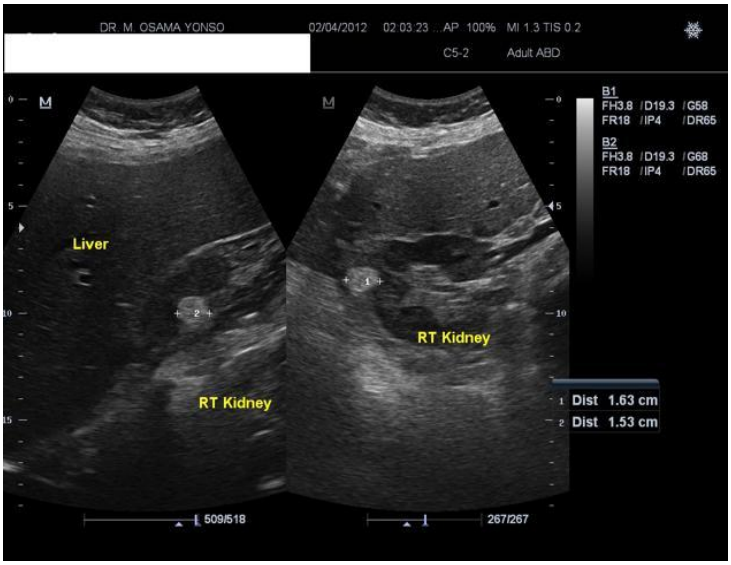

Figure 2.14. *Angiomylipoma (www.google.com).*

Malignant tumors; are much less common in the kidneys than in several other organs, but two are of importance – renal cell carcinoma and nephroblastoma. Secondary tumours are not uncommon, although metastases are neither are frequent nor as numerous as might be expected from the large renal blood flow.

Renal cell carcinoma; (Figure 2.15)**,** renal cell carcinomas account for 90% of all malignant renal tumours in the adult and they have a peak incidence in the sixth

decade. They are often large, and may occur in any part of the kidney. On section, there are usually large areas of dull yellowish tissue, interspersed with vascular, hemorrhagic, cystic and necrotic areas. Although the tumor may often appear to be encapsulated, it is frankly malignant. It commonly grows into the tributaries of the renal vein and may extend along it even into the inferior vena cava. Such venous spread is usually followed by metastases, especially to lungs and bones. Spread also occurs by lymphatics, but often later. Widespread metastases may occur before there are any local sign or symptoms. Invasion and ulceration of the renal pelvis usually causes hematuria (Deam, et al. 2002).

Clinically, hematuria is the most common presenting sign. Loin pain and a palpable mass are other features. Para-neoplastic syndromes are common and related to secretion of hormone-like substances, e.g. hypercalcemia (parathormone), polycythemia (erythropoietin), hypertension (renin) and *Cushing's* syndrome (glococorticoid) (Deam, et al. 2002).

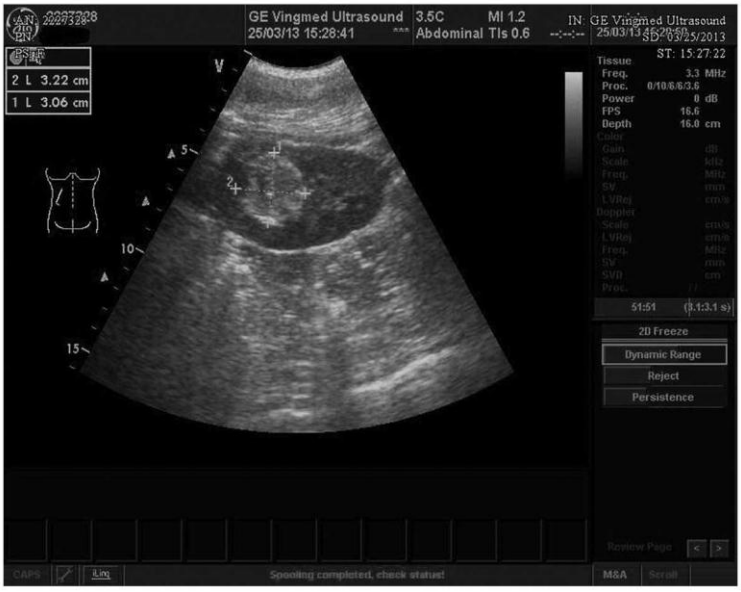

Figure 2.15. *Renal cell carcinoma (www.google.com).*

Nephroblastoma (Wilms' Tumor); this is an embryonic tumor derived from the renal blastema and with features of a rapidly growing sarcoma. It may reach a large size, and though often remaining enclosed within the renal capsule, rapidly invades blood vessels, producing metastases, chiefly in the lungs. It is most common in the first 3years of life. Although rare, it is one of the commonest malignant tumours in childhood and sometimes develops in the fetus and may interfere with delivery (Deam, et al. 2002).

2.3.12 Sickle cell disease of kidneys

SCD is associated with many structural and functional abnormalities of the kidney, which may progress to chronic renal failure and end-stage renal disease. Clinical and pathologic data indicate that intravascular sickling occurs more readily in the kidney than in any other organ (Nath, & Hebbel, 2015).

A series of progressive and random pathologic events involving the kidney begins early in the first decade of life in a patient with SCD and continues throughout life. The combination of hypoxia, hypertonicity, and acidosis in the renal medulla leads to stasis in the vasa recta and to ischemia of the renal medulla and papillary tip, distortion of regional blood flow, focal interstitial nephritis and fibrosis, tubular dysfunction atrophy, and papillary necrosis.

Uric acid nephropathy is a rare condition; it is recurrent and may lead to a radiolucent uric acid stone formation, which can be detected by sonography. Several studies have reported a medullary or diffuse increase in reflectivity on renal sonography in patients with SCD (Attalla, 2010).

People who are known carriers of the disease often undergo genetic counseling before they have a child. A test to see if an unborn child has the disease takes either a blood sample from the fetus or a sample of amniotic fluid. Since taking a blood sample from a fetus has greater risks, the latter test is usually used. Neonatal screening provides not only a method of early detection for individuals

with sickle-cell disease, but also allows for identification of the groups of people that carry the sickle cell trait (Lee et al, 2000).

The terms "sickle-cell crisis" or "sickling crisis" may be used to describe several independent acute conditions occurring in patients with SCD. SCD results in anemia and crises that could be of many types including the vaso-occlusive crisis, a plastic crisis, sequestration crisis, haemolytic crisis, and others. Most episodes of sickle-cell crises last between five and seven days (Best, 2010). "Although infection, dehydration, and acidosis (all of which favor sickling) can act as triggers, in most instances no predisposing cause is identified (Kumar et al, 2009).

The vaso-occlusive crisis is caused by sickle-shaped red blood cells that obstruct capillaries and restrict blood flow to an organ resulting in ischaemia, pain, necrosis, and often organ damage. The frequency, severity, and duration of these crises vary considerably. Painful crises are treated with hydration, analgesics, and blood transfusion; pain management requires opioid administration at regular intervals until the crisis has settled. For milder crises, a sub group of patients manage on NSAIDs (such as diclofenac or naproxen). For more severe crises, most patients require inpatient management for intravenous opioids; patient-controlled analgesia devices are commonly used in this setting. Vaso-occlusive crisis involving organs such as the penis (Olujohungbe, 2013), or lungs are considered an emergency and treated with red-blood cell transfusions. Incentive spirometry, a technique to encourage deep breathing to minimize the development of atelectasis, is recommended (Glassberg, 2011).

2.4 Ultrasound imaging

Renal ultrasonography has become the standard imaging modality in the investigation of kidneys because it offers excellent anatomic detail, requires no special preparation of patients is readily available and does not expose the patient to radiation or contrast agents. Ultrasonography is used to determine the site and size of the kidney and to detect focal lesions like tumors, cysts and renal stones. Furthermore the presence and urodynamic relevance of hydronephrosis can reliably be found. The presence of reno-parenchymatous disease as such is also discernible to the experienced investigator, however most glomerular diseases cannot be further sub classified. Exceptions are primarily reno-vascular disorders like hypertensive nephrosclerosis, diabetic nephropathy or renal vasculitis which can be suspected if the intra-renal resistance index value is increased. Color Doppler sonography in experienced hand allows the reliable detection and quantification of renal artery stenosis and increased resistance index values may indicate irreversible disease (Radermacher, 2005).

2.4.1 Ultrasound physics

2.4.1.1 Properties of Sound Waves

Propagation characteristics: Sound waves have several essential properties:

- Propagation of ultrasound waves: Sound waves travel through air, fluids, and human tissue almost exclusively as longitudinal waves. These are zones in which the molecules that make up the medium are alternately rarefied and condensed. Thus, sound waves must propagate through matter and cannot exist in a vacuum.
- Propagation speed: The speed of sound is relatively slow in all materials (in tissue about 1540 m/s). Consequently, its transit time can be accurately determined by electronic measurements and correlated with the distance traveled by applying the time–distance principle (Schmidt, 2011).

- Reflection (partial or complete) of sound waves at interfaces: The degree of reflection of incident sound waves at an interface depends on the acoustic resistance (“impedance”) of the medium:

- Impedance = the ratio of the incident sound intensity to the portion that is transmitted.

- Acoustic resistance = the product of the density times the speed of sound.

Doppler effect: The Doppler effect states that the frequency of the returning (received) sound waves changes when the source of the sound is moving toward or away from the receiver. According to the time–distance law, the product of time and velocity equals the distance traveled. Thus, the frequency changes in the sound waves reflected from moving red blood cells can be analyzed to determine the direction and velocity of blood flowing through vessels and in the heart (Schmidt, 2011).

2.4.1.2 Resolution

Ultrasound frequency: The quality of an ultrasound examination depends on two criteria relating to the properties of the sound waves:

- The highest possible resolution (high transducer frequency).

- An adequate depth of sound penetration (low transducer frequency).

- Rule: Shorter wavelengths improve resolution but decrease the penetration depth of the ultrasound beam.

- Tradeoff: The optimum frequency range for diagnostic ultrasound is 1-10 MHz. The optimum range of wavelengths is 0.15-1.5mm (Table 2.1).

Table 2.1*.Reference values for resolution and penetration depth as a function of frequency*

Frequency (MHz)	Resolution (mm)		Penetration depth (mm)
	Axial	Lateral	
3.5	1	2	160
5	0.6	1.2	100
7.5	0.4	0.8	50

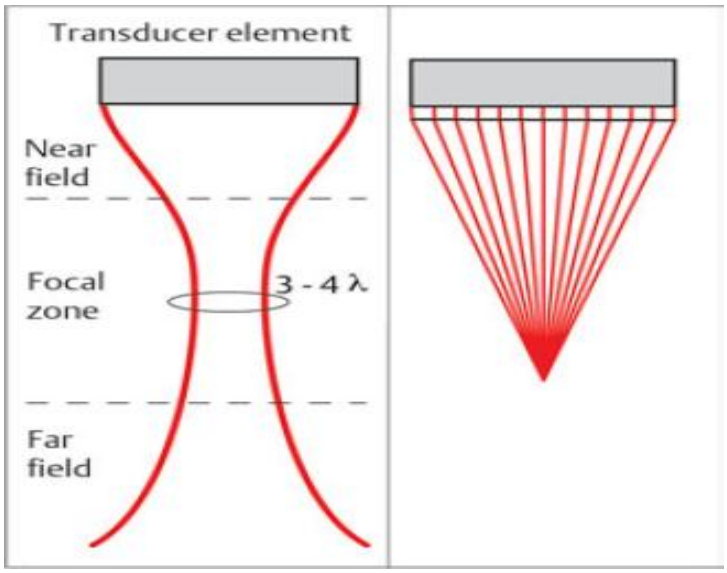

Figure 2.16.*Ultrasound beam shape and electronic focusing (Schmidt, 2011)*

Velocity of sound propagation: This depends on the density of the medium (approximately 1500-1600 m/s in soft tissues and fluids, 331 m/s in air, and 3500 m/s in bone). Ultrasound instruments are calibrated to a mean sound velocity of 1540 m/s.

Axial resolution: sound pulse composed preferably of two (or three) wavelengths is emitted in the longitudinal (axial) direction. The maximum ability to resolve two separate points in the longitudinal direction is equal to one-half the pulse

length, or approximately one wavelength. For example, the resolution at an operating frequency of 3.5MHz is approximately equal to 0.5(-1) mm.

Lateral resolution: The ultrasound beam initially converges with increasing depth, and then widens out again with decreasing intensity and resolution. The focal zone ("waist") of the beam is 3-4 wavelengths wide and is the area where lateral resolution is highest (Figure 2.16). The lateral resolution at a frequency of 3.5MHz is approximately 2mm, meaning that two adjacent points can be distinguished as separate points when they are at least 2mm apart.

Focusing: The purpose of beam focusing in sonography is to achieve maximum resolution and improve the ability to recognize fine details.

- Technical options:

- Make the transducer face concave to produce a convergent beam (concave mirror effect).

- Use a collecting lens.

- Mechanical focusing: This creates a fixed focal zone that cannot be moved (fixed-focus system), although it can be modified somewhat by scanning through a fluid offset.

- Electronic focusing: With this option, the focal zone can be set to any desired depth (Figure 2.16). For example, the focal zone can be positioned to give a sharp image of the gallbladder, or it can be extended over the full depth of the image field.

- Adjusting the focus during an ultrasound examination: This is the hallmark of a proficient examiner. One feature of a high-quality ultrasound system is that a definite change in resolution is seen as the focal zone is moved (Schmidt, 2011).

The propagation of ultrasound waves obeys the laws of wave physics. The following terms have been adopted from radiation optics and wave optics.

Reflection: Sound waves are partially reflected and partially transmitted in biological tissues. An image of an organ is generated from the returning echo signals by analyzing the impedance differences at acoustic interfaces. The higher the acoustic impedance, the greater the degree of reflection, with total reflection occurring at interfaces with a very high impedance mismatch (e.g., between soft tissue and bone, calcium, or air, producing a high-amplitude echo). Interfaces with high acoustic impedance (e.g., gallstones) reflect all of the incident sound and cast an acoustic shadow (Schmidt, 2011).

Scattering: This consists of randomly directed reflections that occur at tissue interfaces and rough surfaces. The echoes generated by scattering centers contribute significantly to medical imaging (e.g., the imaging of rounded organ contours).

Refraction: This phenomenon is most pronounced at smooth interfaces with high acoustic impedance. The sound waves are deflected at an oblique angle relative to the direction of the main beam.

Absorption and attenuation: These describe the “loss” of sound waves due to their spatial distribution in the tissue and the conversion of sound energy to heat. According to the findings of a world health organization (WHO) commission, the conversion of sound energy to heat is within safe limits at the low energy levels used in diagnostic ultrasound. Even so, it is prudent to use the lowest possible ultrasound energy when scanning children and pregnant women. Sound waves are also attenuated in tissues as a result of reflection, scattering, and refraction. This leads to a significant energy loss, which is offset by adjusting the time gain compensation (TGC) on the scanner (Schmidt, 2011).

2.4.2 Ultrasound technique

2.4.2.1 A-Mode, B-Mode, and M-Mode Scanning

A-mode scanning (Figure 2.17a): In this technique the amplitudes (A-mode) of the echo signals returned from tissue interfaces are displayed as a series of amplitude deflections along a horizontal axis, as on an oscilloscope.

B-mode scanning (brightness mode, Figure 2.17b):

- Principle: Reflected ultrasound pulses are displayed on the monitor as spots of varying brightness in proportion to their intensity. The sound waves are transmitted into the tissue in a parallel scan or a fan-shaped beam, and the echoes are reflected back to the transducer and assembled line-by-line according to their arrival time.

- Signal display and image reconstruction: Approximately 120 image lines are assembled to make a two-dimensional sectional image. The various echo intensities are converted by electronic processing into image spots of varying density or shades of gray (gray-scale display, brightness modulation).

M-mode scanning (time. motion): This technique generates a time-motion trace that records the motion of acoustic reflectors such as heart valves and myocardial walls over time (Schmidt, 2011).

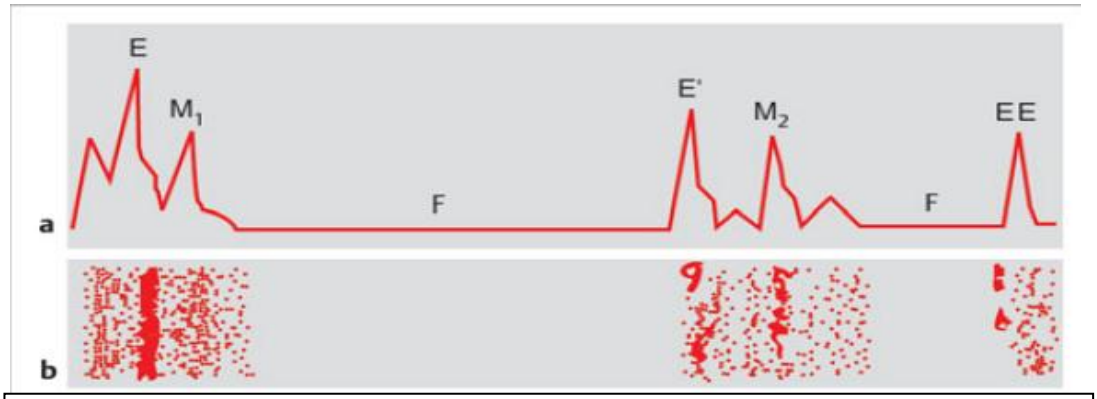

Figure 2.17 a, b A-mode and B-mode scans, illustrated for the maxillary sinus. a A-mode signal. b echoes (bone), El = entry echo (bony ridge or polyp), M1 = mucosa, M2 = thickened mucosa, F = fluid, EE = exit echo (Schmidt, 2011).

2.4.2.2 Doppler and Duplex Sonography

Continuous-wave (CW) Doppler: Two piezoelectric crystals are used, one for the continuous transmission of ultrasound pulses (continuous wave) and one for the reception of reflected ultrasound signals.

The frequency spectra of returning echoes are displayed acoustically and also visually if desired. The frequency shifts can be used to calculate the direction and velocity of blood flow. This technique does not, however, provide information on the depth or range of the echo source.

Pulsed Doppler: This technique employs one piezoelectric crystal that functions alternately as a transmitter and receiver (pulsed wave).

Echo signals are recorded from a designated sample volume during the receiving phase of the scan. This makes it possible to determine the depth and width of the sample volume and investigate blood flow within a circumscribed area.

Duplex sonography: CW or pulsed Doppler is combined with B-mode imaging, providing visual feedback for positioning the Doppler beam and the sample volume.

Power Doppler: This technique demonstrates the spatial distribution of blood flow but cannot determine flow direction. It is most useful in establishing the presence or absence of vascularity and evaluating the quantity of blood flow. Power Doppler is excellent for detecting increased vascularity due to inflammation, for example.

Spectral Doppler: The spectral analysis of blood flow patterns is used to determine the time course and velocity distribution of the flow, i.e., its mean and maximum velocities. This is of key importance in the diagnosis of vascular stenosis (Schmidt, 2011).

2.5 Previous studies

Many studies were published to show sonographic evaluation of renal morphologic and physiologic finding worldwide. Some countries have already established their normal renal length and volume; some of these studies were conducted to provide reference values for renal size, blood flow indices and echogenicity so as to differentiate between normal and abnormal Kidneys early and quickly by using ultrasound. Therefore, these data could be important to diagnose the problem in kidneys easy and to give the suitable treatment in a short time.

Ibinaiye et al, (2013) they found renal size in the study group was compared with that of the control group and was found to show a significant increase (Table 2.2). The mean right renal length in the study group and control group was 10.65±0.97 cm and 9.95±0.80 cm (P<0.001), respectively, whereas the mean left renal length in the study group and control group was 10.70±1.02 cm and 10.00±0.66 cm (P<0.001), respectively. The mean right renal AP diameter in the study group and control group was 4.45±0.54 cm and 4.01±0.30 cm (P<0.001), respectively, whereas the mean left renal AP diameter in the study group and control group was 4.65±0.47 cm and 4.17±0.47 cm (P<0.001), respectively. The mean right renal transverse diameter in the study group and control group was 7.11±0.73 cm and 6.00±0.49 cm (P<0.001), respectively, whereas the mean left renal transverse diameter in the study group and control group was 7.17±0.76 cm and 6.07±0.51 cm (P<0.001) respectively. The mean right renal parenchymal thickness in study group and control group was 1.90±0.26 cm and 1.50±0.12 cm (P<0.001), respectively, whereas the mean left renal parenchymal thickness in the study group and control group was 1.95±0.19 cm and 1.55±0.14 cm (P<0.001), respectively. However, all the three patients above 50 years had

reduced renal size when compared with four patients of the control group who were also above 50 years.

Table 2.2. *Assessment of kidney size in patients and controls.*

Study parameter	Study group *n*=74				Control group *n*=20				Level of significance	
	Right kidney		Left kidney		Right kidney		Left kidney			
	Range	Mean	Range	Mean	Range	Mean	Range	Mean	Right	Left
Length (cm)	8.5-13.4	10.65±0.97	8.3-14.2	10.70±1.02	8.6-11.3	9.95±0.80	8.8.8-11.4	10.00±0.66	<0.000111	<0.0001
Anterior posterior diameter (cm)	3.4-5.7	4.50±0.54	3.2-5.7	4.65±0.47	3.6-4.6	4.01±0.30	3.5-5.6	4.17±0.47	<0.0001	<0.0001
Transverse diameter (cm)	5.7-8.8	7.11±0.73	4.8-8.6	7.17±0.76	5.0-6.9	6.00±0.49	5.2-7.0	6.07±0.51	<0.0001	<0.0001
Parenchymal thickness (cm)	1.2-2.7	1.90±0.26	1.5-2.5	1.95±0.19	1.3-1.7	1.50±0.12	1.3-1.9	1.55±0.14	<0.0001	<0.0001

Adeela et al, (2011) in their study (comparison of renal size among different ethnicities) were used two dimensional ultrasound machine for one hundred university students to assess the renal size. Before, starting the exam, height and weight were taken. The image was taken in supine position. The mean length for the right and left were 9.7cm, and 9.9 cm respectively. The mean width was 5.6 cm and 6.09 for the right and left respectively.

Balci et al, (2008) they found the most frequent US findings (expressed as percentages of all patients) were hepatomegaly (71.6%), renal enlargement (30.4%), autosplenectomy (33.3%), cholelithiasis (30.4%) and splenomegaly (17.4%). A bright liver was identified in 6 patients (5.9%), an echogenic pancreas in 4 patients (3.9%), and pancreatic punctate echogenic foci were identified in 5 patients (4.9%). Medullary or diffusely increased renal echogenicity was observed in 16 patients (15.7%). Sonographic findings typical of renal papillary necrosis were observed in one patient with S/S. Periportal lymphadenopathy was detected in 10 (11.9%) of 84 patients of the S/S group, and 2 (11.1%) of 18 patients of S/ßthal group.

A study by Brandt et al, (1982) (ultrasound assessment of renal dimensions) in (Chicago), confirms the accuracy and reliability of sonographic assessment of renal size. They showed that sonographic dimensions are smaller than those obtained radiology. With improve position, the mean renal length was found to be 10.7 cm in the right side and 11.1cm in the left side (Table 2.3) & (Table 2.4).

Table 2.3. *Right renal dimensions in sample group of patients examined prospectively.*

	Mean	***STDEV***
Length		
Oblique	10.90	0.83
Prone	11.06	0.81
Depth (anteroposterior)		
Oblique	4.8	0.3
Prone	5.0	0.1

Table 2.4. *Left renal dimensions in sample group of patients examined prospectively.*

	Mean	***STDEV***
Length		
Oblique	11.19	0.87
Prone	11.23	0.71
Depth (anteroposterior)		
Oblique	5.0	0.3
Prone	5.0	0.4

Emamian et al, (1993) was performed on 665 adult volunteers using renal sonography. It showed a median renal length 11.2 cm on the left side and 10.9cm on the right side. The median renal volume was 146 cm3 on the left side and 136cm3 in the right. Renal size was found to be decreased with age, increased due to parenchymal reduction (Table 2.5).

Table 2.5. *Renal Measurements at Sonography in 665 Volunteers.*

Measurements	Age (yr)					Women	Men	All
	30	40	50	60	70			
No. of subjects								
Women	68	82	95	75	38	358	0	358
Men	53	62	73	87	32	0	307	307
Renal length (mm)								
Left	115 (104, 128)	113 (103, 123)	113 (102,125)	111 (100, 122)	105 (94, 120)	110 (99, 121)	115 (104, 126)	112 (101, 123)
Right	111 (101, 124)	112 (100, 123)	110 (100, 122)	108 (95, 120)	104 (91, 118)	107 (95, 120)	112 (101, 124)	109 (98, 122)
Renal width (mm)								
Left	59 (51, 66)	58 (50, 65)	58 (53, 65)	58 (51, 65)	56 (49, 62)	56 (49, 62)	60 (53, 68)	58 (51, 65)
Right	58 (50, 66)	58 (52, 66)	58 (52, 64)	57 (50, 64)	55 (50, 63)	56 (50, 61)	59 (53, 66)	57 (51, 64)

Glodny et al, (2009) in their study "normal Kidney size and its influencing factors" were applied normal ultrasound values for pole-to-pole kidney length. Cortical size was also recorded. The length was 10.8 cm for the right and 11.13 for the left kidney. The cortical size was same in the right and in the left (6.6mm) the most significant independent predictors for the length and cortical size were body size, Body mass index age and gender.

Mazin et al, (2014) in their study entitled (Establishment of Reference Values for Renal Length and Volume for Normal Adult Sudanese using MRI Disc Summation Method) The study showed that the kidneys length measured for normal Sudanese subjects were 10.08±0.46, 10.67±0.47 for right and left, respectively. The mean volumes were 101.6 cm^3 and 104 cm^3 for right and left kidney, respectively (Table 2.6).

Table 2.6. *Mean Standard deviation of Kidneys volume, and length for the total sample.*

Descriptive Statistics					
Parameters	*N*	*Min*	*Max*	*Mean*	*STDEV*
Right Kidney Volume(Cm^3)	98	80.32	122.91	101.6	12.98
Right Kidney Length(Cm)	98	9.00	11.25	10.18	0.46
Left Kidney Volume (Cm^3)	98	82.56	126.54	104.0	12.99
Left Kidney Length(Cm)	98	9.00	11.70	10.67	0.47

Mujahid et al, (2011) in their study "ultrasonographic assessment of renal size and volume and its correlation with BMI in adults" assessed renal size by ultrasound in 4.035 adult subjects without renal disease. The mean renal length on the right side was 10.16cm, width as 4.2 and thickness was 4.4 cm. on the left side the mean length was 10.27, width was 4.4 and thickness was 5.1cm. The mean renal volume on the right was 99.8 cm3 and 124cm3 on the left (Table 2.7). The study concluded that the volume in the left side was significantly larger than the right in both gender.

Table 2.7. *Renal dimension in males and females.*

	Males (n=1,961)				Females (n=2,074)			
	Right kidney		Left kidney		Right kidney		Left kidney	
Parameters	Mean±SD	Range	Mean±SD	Range	Mean±SD	Range	Mean±SD	Range
Renal length (mm)	103.2±8.9	70–131	104.6±9.1	80–137	100.0±8.59	77–131	100.9±8.97	80–126
Renal width (mm)	45.3±7.3	19–74	50.5±6.6	23–69	40.2±5.96	23–69	44.9±6.27	26–65
Renal volume (cm^3)	113.0±39.4	27.2–270.8	140.7±41.5	30.8–246.3	87.4±30.14	30.8–246.3	108.8±34.8	35.9–251.3
Parenchymal thickness (mm)	9.0±3.1	29.0-5.1	15.8±3.2	8.0–29.0	13.8±2.64	8.0–29	14.5±2.8	27–14.5
Relative renal length	0.60±0.05	0.45–0.81	0.6±0.05	0.49–0.85	0.65±0.056	0.49–0.85	0.65±0.059	0.82–0.65

Shin et al, (2009) measured the kidney volume with Multi-Detector Computed Tomography Scanning in Young Korean to estimate the normal kidney volume of healthy young Korean men and evaluated its predictability of renal function and relationship with body indexes. Their study included 113 patient Images were obtained prior to and after the administration of 150 mL of iodinated contrast media during the parenchymal phases of enhancement. The kidney size was measured using GE Advantage Windows Workstation, and kidney length was measured using coronal sections. Maximum kidney length was calculated from all coronal sections. The kidney volume was measured from contiguous slices. In coronal section images with parenchymal enhancement, the region of interest was drawn around the kidney, and the slices were reconstructed at 1-mm intervals to obtain a 3-D volume-rendered image of the kidney. The volume was

calculated by multiplying the sum of areas from each slice by the reconstruction interval at the workstation. Their results showed that the mean kidney volume was 205.15 cm2 (138.53-359.6 cm2). The left kidney was significantly ($p < 0.05$) larger than the right kidney, and they were highly correlated (correlation coefficient: $r = 0.874$, $p < 0.05$). The mean kidney length was 108.02 cm (9.09-12.49 cm). The left kidney was also significantly ($p < 0.05$) longer than the right kidney. The kidney length and kidney volume were highly correlated reciprocally ($r = 0.671$, $p < 0.05$) (Table 2.8).

Table 2.8. *Mean Value of Kidney Length and Volume According to Position.*

Parameters	*Length (cm)*	*Volume (cm3)*
Lt. Kidney	10.90 ± 0.72*	207.32 ± 37.50
Rt. Kidney	10.70 ± 0.76	203.26 ± 38.60
Both Kidney	10.80 ± 0.69	205.15 ± 37.13

*$p < 0.05$ vs. Rt kidney length, $^{\dagger}p < 0.05$ vs. Rt kidney volume (± Data presentedare Mean ± SD).

Zeb et al, (2012) in their work entitles sonographic measurement of renal dimensions in adults; a survey to establish age and sex based diagnostic reference values in Pakistan. The study assessed the normal range of values for renal dimensions in a symptomatic adult population with various age groups. The mean kidneys lengths were 9.7 cm on right side and 10cm on the left side. The mean width was 4.6 cm, cortical size was 1.46 cm with estimated average kidney volume was 135.7 cm3 (Table 2.9).

Table 2.9. *Renal measurements with normal eGFR. Mean (with 95% confidence intervals).*

	Age (yrs)					Sex		All
Measurements	30-39	40-49	50-59	60-69	70 & above	Males	Females	
Subjects- males		38	40	11	12	147	0	147
females	45	21	22	15	3	0	78	78
	17							
Right Length (cm)	9.94 (9.7-10.1)	9.83 (9.66-10.0)	9.92 (9.71-10.1)	9.82 (9.55-10.1)	9.22 (8.81-9.64)	9.82 (9.69-9.96)	9.88 (9.72-10.0)	9.85 (9.74-9.95)
Left Length (cm)	10.0 (9.81-10.3)	10.3 (10.0-10.5)	9.99 (9.78-10.2)	9.85 (9.50-10.2)	9.13 (8.69-9.57)	10.1 (9.90-10.2)	9.92 (9.74-10.1)	10.0 (9.85-10.1)
Right Width (cm)	4.42 (4.24-4.61)	4.46 (4.28-4.64)	4.37 (4.21-4.53)	4.37 (4.07-4.67)	4.03 (3.69-4.38)	4.52 (4.41-4.63)	4.13 (3.98-4.29)	4.39 (4.30- 4.48)
Left Width (cm)	4.96 (4.80-5.11)	4.89 (4.71-5.07)	4.75 (4.59-4.91)	4.74 (4.48-5.01)	4.35 (4.06-4.64)	5.03 (4.93-5.13)	4.42 (4.29-4.56)	4.82 (4.73- 4.90)
Right renal volume (cm^3)	33.4 (31.1-35.8)	32.1 (29.5-34.7)	33.3 (30.6-36.0)	32.2 (28.3-36.1)	26.1 (22.6-29.7)	33.6. (31.9-35.2)	30.2 (28.1-32.3)	32.4 (31.1-33.7)
Left renal volume (cm^3)	41.4 (38.4-44.2)	39.9 (36.9-42.9)	39.0 (35.9-42.0)	36.5 (31.5-41.5)	29.7 (24.6-34.8)	41.8 (39.8-43.8)	33.6 (31.5-35.6)	39.0 (37.4-40.5)

Rosado et al, (2014) in their study (Sickle cell anemia - a review of the imaging findings) concluded that the kidney is also susceptible for sickling of red blood cells and infarction, especially in the medulla, where vasa recta flow through a hypertonic interstitium. Capillary obliteration result in medullary and papillary necrosis. At imaging, up to 50% of patients have enlarged kidneys. At ultrasonography kidneys may have normal echogenicity, may be diffusely hyperechogenic or may have increased medullary echogenicity with normal cortical echogenicity (Figure 2.18). Later in life, if renal failure develops, kidneys become small and hyperechogenic.

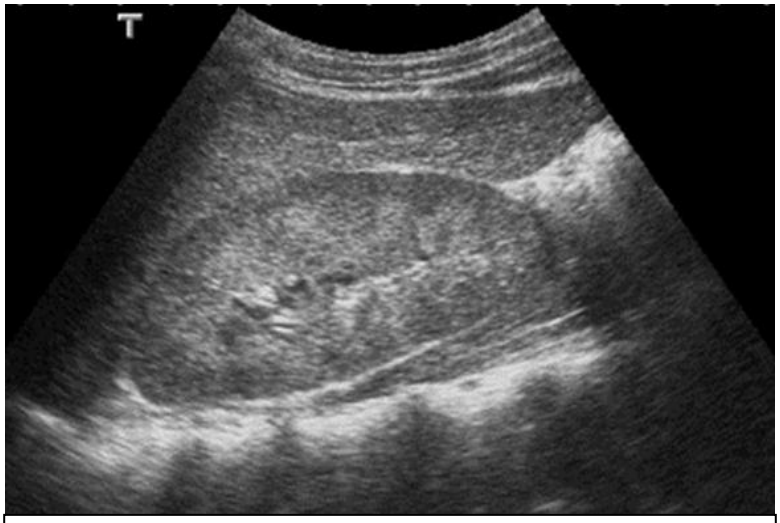

Figure 2.18.*Shows an enlarged right kidney with hyperechogenic medulla in an 11years boy with SCD (Rosado et al, 2014).*

Ibinaiye et al, (2013) Concluded that medullary and diffuse renal hyperechogenicity was observed in 14 (18.9%) and 7 (9.5%) patients, respectively (Figure 2.19). Ultrasound findings consistent with renal papillary necrosis, viz-a-viz multiple round or triangular cystic spaces communicating with the collecting system in the medullary region without dilated renal pelvis

was observed in one patient (Figure 2.20); the intravenous urogram (Figure 2.21) confirmed papillary necrosis in this patient. A left hydronephrosis was noted in one patient.

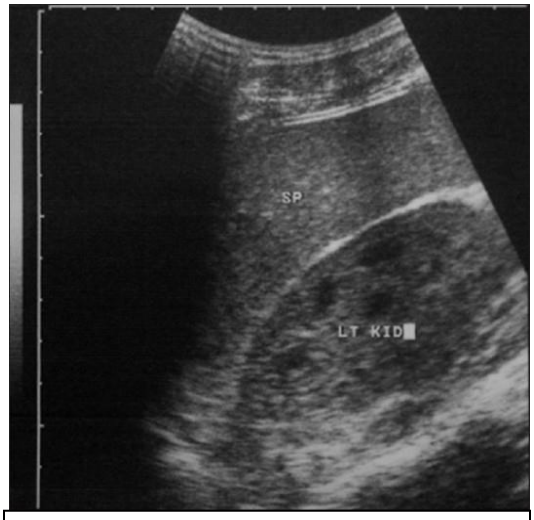

Figure 2.19. *Shows diffuse increase in renal echotexture similar to that of the adjacent liver, in a 38-year-old female patient with SCD (Ibinaiye et al, 2013).*

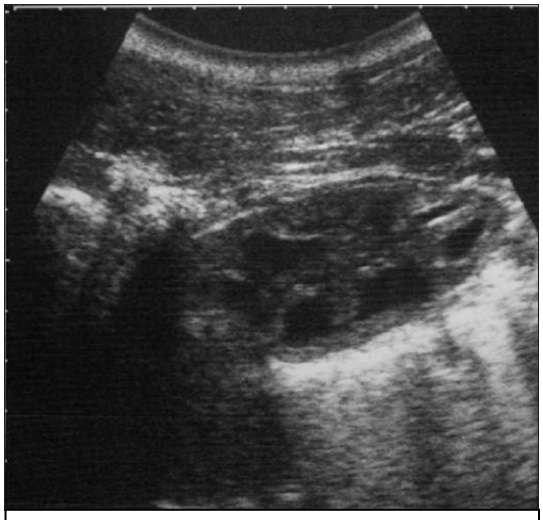

Figure 2.20. *Shows triangular fluid-filled cavities within renal papillae that communicate with PCS in an 18 years male patient with SCD (Ibinaiye et al, 2013).*

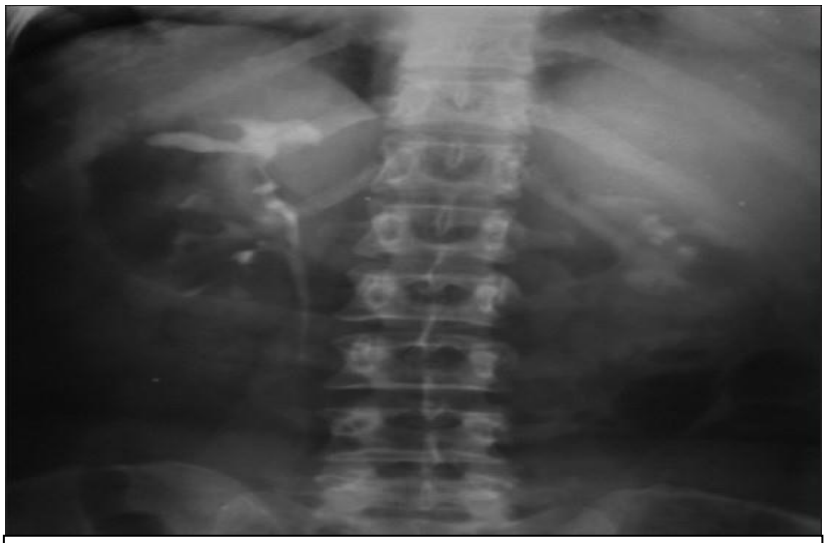

Figure 2.21. *Urogram of the patient described in (**Figure 18**) showing corresponding changes in the upper pole calyces compatible with papillary necrosis.adjacent liver, in a 38 years female patient with SCD.(Ibinaiye et al, 2013).*

Morghazi et al, (2005) Echogenicity showed the strongest correlation with all 4 histologic parameters (r = 0.28-0.35). Renal size was significantly correlated with glomerular sclerosis (r = −0.26) and tubular atrophy (r = 0.20). Parenchymal thickness, but not cortical thickness, correlated with tubular atrophy (r = −0.23). By multivariate analysis, tubular atrophy and interstitial inflammation, but not interstitial fibrosis, were significant determinants of cortical echogenicity. Severe chronic disease (>50% sclerosed glomeruli or a score of 3 out of 5 or greater for tubular atrophy or interstitial fibrosis) was present in 69% and 47% of patients with combined renal length <20 cm and >20 cm, respectively (P = <0.05). For cortical echogenicity >1.0 (>liver echogenicity) and ≤1.0, the proportions of severe disease were 66% and 30%, respectively (P < 0.001). Severe disease was present in 86% of patients with combined renal length <20 cm and cortical echogenicity >1.0 (Table 2.10).

Table 2.10. *Sonographic findings*

	Length *cm*			Cortical echogenicity	Cortical thickness	Parenchymal thickness
	Left	Right	Diff.[a]	Kidney/liver	*mm*	*mm*
Mean	10.9	10.9	0.7	1.04	8.3	17.1
Median	11.0	11.0	0.6	1.02	8.2	16.3
Range	7.5–15.0	7.6–14.5	0–4.6	0.71–1.89	4.7–12.5	7.0–33.7
N	205	207	205	168	137	145

Jagdeesh et al, (2013) in their study entitled " Correlation of ultrasonographic parameters with serum creatinine in Chronic Kidney Disease revealed" it revealed that Renal echogenicity and its grading correlates better with serum creatinine in CKD than other sonographic parameters like longitudinal size (P =

0.085), parenchymal thickness (P = 0.046), and cortical thickness (P = 0.656) (Table 2.11). As serum creatinine is an indicator of kidney function, renal echogenicity is a better parameter to estimate renal function with the added advantage of irreversibility when compared to serum creatinine, which improves with kidney replacement therapy like -hemodialysis, peritoneal dialysis, and renal transplantation in chronic kidney disease.

Table 2.11.*Statistical correlation between serum creatinine and mean longitudinal size, mean parenchymal thickness, and mean cortical thickness.*

Correlations			
	Serum creatinine (mg/dl)		
	Correlation	*P* value	*N*
Mean longitudinal size (mm)	−0.224	0.085	60
Mean parenchymal thickness (mm)	−0.259	0.046	60
Mean cortical thickness (mm)	−0.060	0.656	57

N: No of patients, *P* value: Level of significance

Papadaki et al, (2003) at the time of the examination, 41% of the patients had undergone splenectomy and 23.8% had undergone cholecystectomy. The most frequent US findings (percentages refer to all patients) were: hepatomegaly (70.5%), splenomegaly (48.6%) and cholelithiasis (20%). A bright liver was identified in 3.8% and focal hepatic lesions were present in two patients of the TI group. Functional disorders of the gallbladder concerned mainly patients with sickle-cell syndromes. Of those with S/S, 30.8% had a shrunken spleen. An echogenic pancreas was identified in one patient in each group. Increased renal echogenicity was observed in 17.6% of patients with sickle-cell syndromes. One case of polycystic kidney disease was diagnosed and coexisted with S/S.

Heine et al, (2005) Transplant recipients with high coronary risk had higher intrarenal resistance indices than low-risk patients. Higher age, female gender, and lower body mass index were independently associated with increased resistance indices. Renal resistance indices were correlated with common carotid intima-media thickness RI: r = 0.270 (P = 0.005); PI: r = 0.355 (P < 0.001).This association remained significant after adjusting for renal function. Renal resistance indices were increased in patients with pathologic ankle-brachial-indices compared to patients with physiologic ankle-brachial-indices [RI: 73.3 ± 7.1 vs. 70.2 ± 6.9 (P = 0.03); PI: 146.4 ± 29.9 vs. 131.4 ± 25.9 (P = 0.01)]. Renal resistance indices were neither significantly correlated with (GFR), nor with donor age.

Guvenc et al, (2005) the 60 patients with homozygous SCD who entered the study were divided into 2 groups. Group 1 included 45 patients who were living in steady-state conditions and had no history of transfusions within the 3 months before the initiation of the study. Group 2 consisted of 15 patients with signs of painful vaso-occlusive crisis during evaluation. Group 2 patients had significant reductions in 3 measures of flow velocity in both main renal arteries, compared with group 1 patients ($P < .04$, $P < .001$, and $P < .01$). Mean & end-diastolic velocities in the segmental arteries ($P < .01$, and $P < .001$, respectively) and end-diastolic velocities in the interlobar arteries ($P < .04$) were lower in group 2 patients than in group 1 patients. Analysis of resistive (RI) and pulsatilty (PI) indices in the investigated arteries demonstrated that the RI of the renal ($P < .001$; $P < .0001$), segmental ($P < .002$; $P < .0001$) and interlobar ($P < .001$; $P < .0001$) arteries of both kidneys in group 2 patients were significantly higher than the RI in group 1 patients and the control subjects, respectively. Total PI ($P < .003$; $P < .0001$) and total RI ($P < .0001$; $P < .0001$) for both kidneys were markedly higher in group 2 patients than in group 1 patients and the healthy

subjects, respectively. Our preliminary results suggest a reduction of renal blood flow and an increase in renal vascular resistance during painful crisis compared with steady-state SCD.

Lin et al, (2003) investigated the influence of age on intra-renal arterial resistive index (RI) measurement in 135 normal subjects (71 male, 64 female; age range = 17-68 years, median age = 37 years). They found that although there is a statistically significant positive correlation between intra-renal RI and age, the correlation is weak. This suggests that the influence of age on RI measurement is small and may be of no clinical importance.

Ohta et al, (2005) evaluated the relationship between these indices and pulse wave velocity (PWV), a measure of arterial stiffness, which reflects atherosclerosis, and determined whether renal RI and PI differ depending on the underlying renal disease. A total of 245 in patients with or without renal impairment who underwent ultrasonographic assessment of the renal artery were enrolled in the study. Patients with renal artery stenosis or severe renal failure (serum creatinine > or=6 mg/dl) were excluded from the study. They concluded that these results suggested that the increased RI of the renal arteries is associated with the severity of systemic atherosclerosis. Furthermore, the intra-renal vascular resistance differs depending on the underlying renal disease, and appears to increase to a greater extent in diabetic nephropathy.

Jorg et al, (2002) prospectively tested the hypothesis that a high renal resistance index (≥80) predicts progression of renal disease in patients without renal artery stenosis. In 162 patients newly diagnosed with renal disease, the resistance index (1-[end diastolic velocity/ maximum systolic velocity]*100) was measured in segmental arteries of both kidneys. Creatinine clearance was measured at baseline, at 3, 6, and 12 months, and then at yearly intervals there after (mean follow-up 3±1.4 years). The combined endpoint was a decrease of creatinine

clearance by ≥50%, end-stage renal disease with replacement therapy, or death. Twenty-five patients (15%) had a renal resistance index value ≥80 at baseline. Nineteen (76%) had a decline in renal function; 16 (64%) progressed to dialysis, and 6 (24%) died. In comparison, in patients with renal resistance index values <80, 13 (9%) had a decline in renal function, only 7 (5%) became dialysis-dependent, and 2 (1%) died (P<0.001). In a multivariate regression analysis, only proteinuria and resistance index were independent predictors of declining renal function. A renal resistance index value of ≥80 reliably identifies patients at risk for progressive renal disease.

Chapter three
Materials and methods

3.1. Materials

3.1.1 Patients:

The study was an experimental clinical study carried out in West of Sudan-Kordofan state at Kuwaiti Pediatric Hospital, Modern Health Insurance Centre in Obaied city, and Dr. M. A. Mageed Medical Complex in El-nohood city. The study started in August 2014 and finished in April, 2017, in which a group of (115) patients with sickle cell disease with different age and gender were drown for renal US examination. Another group of (100) healthy volunteers were selected as a control group and gray scale and Doppler US procedure was done for them in order to establish some preliminary data of the population. Patients with sickle cell disease of duration less than (3) years were excluded in order to give an opportunity for renal changes in size and parenchyma to appear.

3.1.2 Machines:

Two US machines were used in the study; the first one was Accuvixxg-Avxgl30-samsung-Korea (Figure 3.1), and the second one was Mindary DC-N6-China (Figure 3.2). The probe which was used was curve linear multi hertzs probe. An US gel was used and it was put at the top of the transducer to avoid reflection of ultrasound and to maintain a good transmission of US beam inside the body.

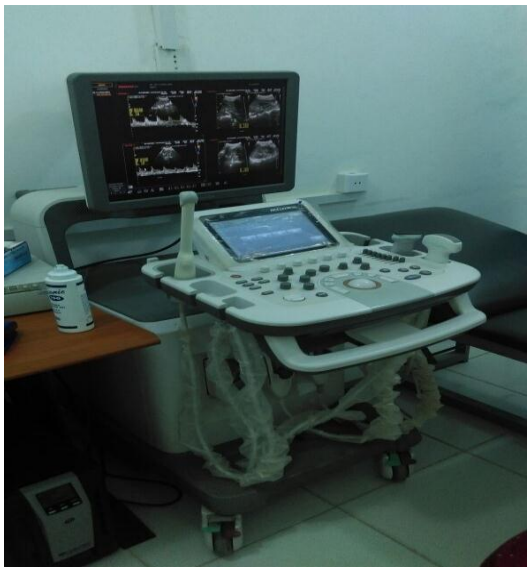

Figure 3.1. *Accuvixxg-Avxgl30-samsung-Korea (Health Insurance Centre, Obaied,Sudan)*

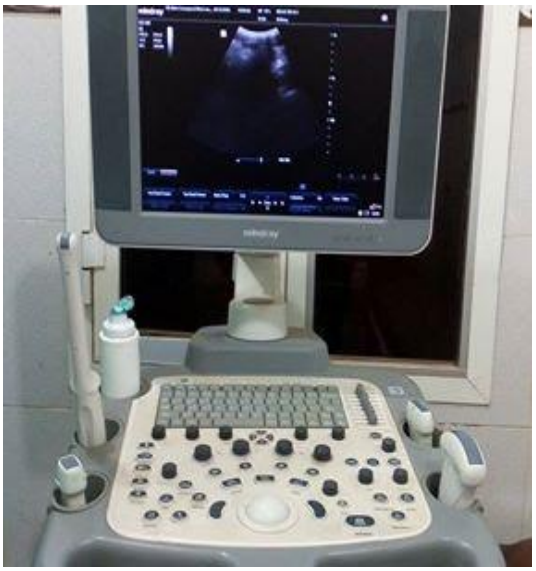

Figure 3.2.*Mindary DC-N6 -China (Dr.M. A.elmageed Centre, El-nehood, Sudan)*

3.2. Methods

3.2.1 Technique:

The examination began with subject supine. The para-aortic region was examined to exclude the presence of horse show kidneys. Length, width, and thickness of the kidneys were measured. The longitudinal dimensions of the kidneys were measured in a section visually estimated to represent the longest longitudinal section. Both lower and upper poles were defined. Coronal or sagittal view with the patient in decubitus position obtained in case of difficulty of long axis of the kidney with the patient supine. The patient was asked to elevate the ipsilateral arm above the head and take a deep breath and hold it to have a good view for both poles. Supero-inferior (pole to pole) measurement was taken in that view, and then the width and depth were measured in a section perpendicular to the long axis of the kidney as assessed from the longitudinal image. The probe was thus not necessary perpendicular to the skin. The transverse section was intended to be placed quite close to the hilum of the

kidney but at the same time free of pelvis. Width and depth were then measured in two orthogonal directions; renal volume was estimated from the three orthogonal measurements on the base of ellipsoid formula (Volume= $L \times W \times AP \times 0.523$).

The echogenicity of the cortex for each kidney was compared with the liver in the right side and spleen in the left side to detect echogenicity changes.

All patients underwent duplex ultrasonography for estimation of renal arterial resistance index and pulsatilty index. The patients were examined in supine, right decubitus and left decubitus positions. A colour Doppler followed by pulse wave Doppler. (PW) modes were applied for the spectral analysis and determination of renal arterial (RI & PI) value which obtained from kidneys.

3.2.2 Image presentation

Ultrasound images were presented and diagnosis confirmed with my colleagues Mr. Omar Abdelmageed (Dr. M. A.elmageed Medical Complex, Alnohood-Sudan), Mr. Abdelrahman Mohamed Ali (Eithar Medical Complex, Obaied - Sudan), and Mr. Fath Elrhman Omar Abdalla (Health Insurance Modern Centre, Obaied - Sudan).

3.2.3 Statistic studies

Excell 2010 was used to analyse the data to find the significant difference between variables of patients with sickle cell disease and control group, in addition to linear relationship between body characteristics and blood flow indices.

Variables used for data collection are age, gender, weight, height, BMI, kidney length, width and thickness, kidney volume, RI & PI for renal arteries, and the kidney echogenicity.

3.2.4 Ethical consideration

The researcher got an ethical approval from Sickle Cell Disease Centre - Sudan and hospitals in which the study was carried out to collect the data from the patient for the research and verbal consent from the patient and their relatives.

Chapter Four
Results

The following chapter will highlight the results related to SCD patient and control group in view of bars and tables, correlation and ultrasound images specifically: incidence of SCD based on gender, SCD echogenicity, kidneys volume (SCD, control), correlation of age and BMI versus RI/PI, and the kidneys volume versus age, BMI and RI/PI.

Table 4.1.*Mean and Standard deviation of age, and BMI for SCD patients and control group.*

Parameters	***Mean***	***STDEV***
Age/ Patients	10.5	4
BMI/ Patients	16.8	3
Age/ Control Group	17	4.9
BMI/ Control Group	23.2	5.5

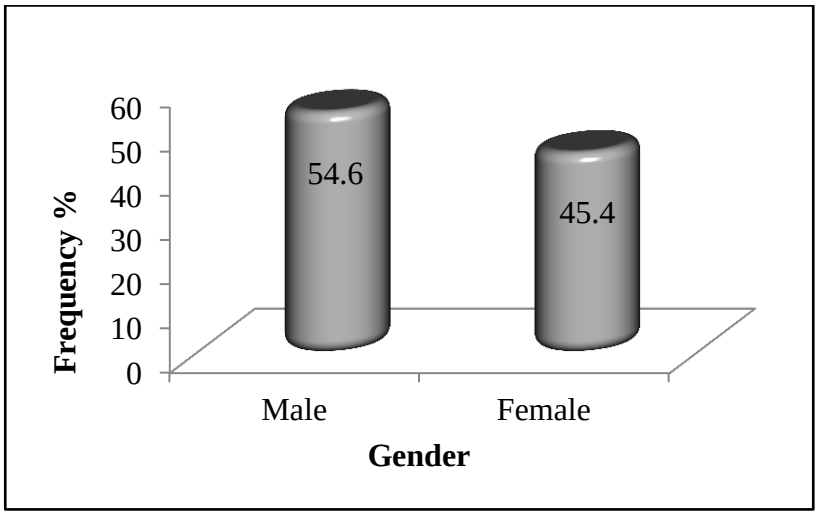

Figure 4.1.*Gender frequency of SCD patients.*

Table 4.2.*Mean and STDEV of Kidneys volume, and length for SCD patients & control group.*

Parameters	***Mean***		***STDEV***	
	Pat	Cont	Pat	Cont
Right Kidney Volume(Cm^3)	59.41	97.85	2.21	29.53
Right Kidney Length.(Cm)	8.78	9.14	5.22	1.04
Left Kidney Volume (Cm^3)	98.38	100.2	21.38	22.73
Left Kidney Length(Cm)	8.93	9.5	5.22	1.04

Table 4.3.*Mean and STDEV of RI & PI for Rt & Lt RAs for SCD patients & control group.*

Parameters	***Mean***		***STDEV***	
	Pat	Cont	Pat	Cont
Right renal artery resistive index	0.8	0.7	0.2	0. 1
Right renal artery pulsatilty index	1.5	1.4	0.4	0.4
Left renal artery resistive index	0.77	0.7	0.2	0.1
Left renal artery pulsatilty index	1.6	1.5	0.2	0.5

Table 4.4.*Frequency of echogenicity of kidneys in patients with SCD.*

Characteristics	***Frequency***	***Percent***
Echogenicity of the right kidney		
hyperechoic	42	36.5%
Normal echogenicity	73	63.5%
Echogenicity of the left kidney		
Hyperechoic	43	37.4%
Normal echogenicity	72	62.6%

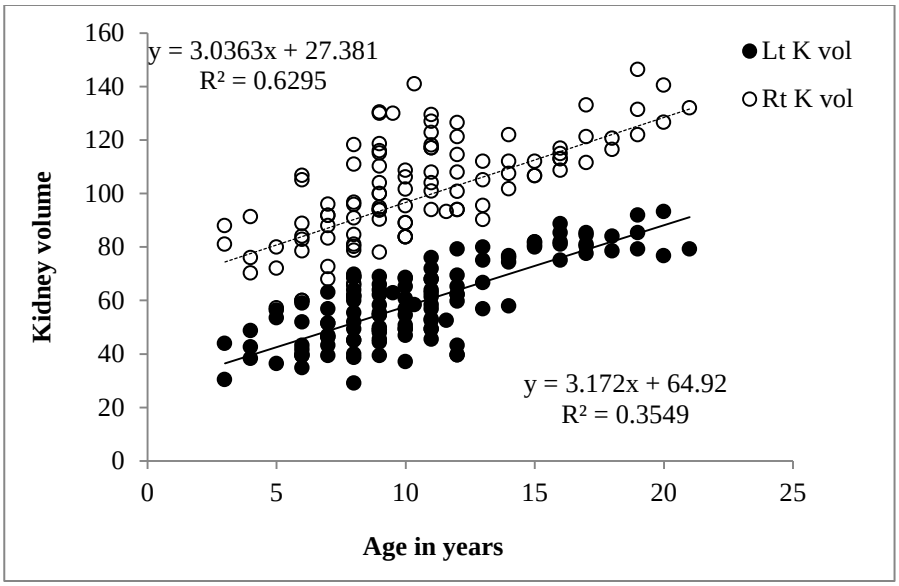

Figure 4.2.*Scatter plot shows the correlation of age in years with Rt & Lt kidney volume among patient with SCD.*

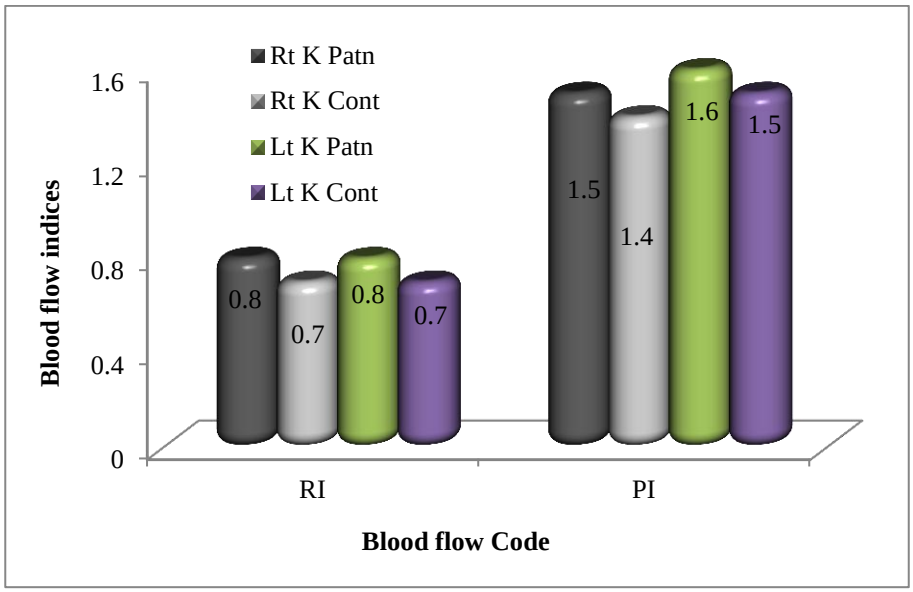

Figure 4.3.*Shows the blood flow indices variation among SCD patient and control group.*

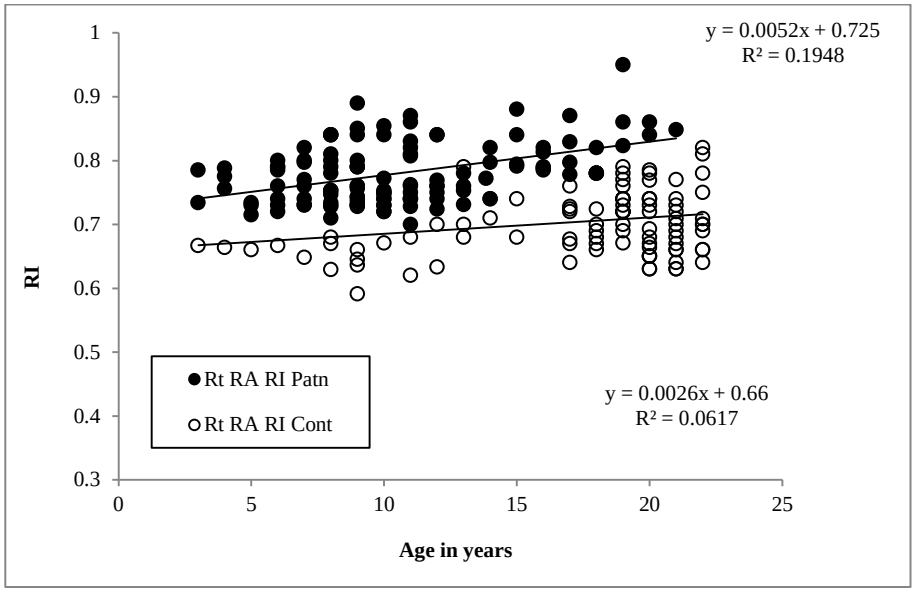

Figure 4.4.*Scatter plot shows the correlation of age in years with Rt renal Artery RI among patient and control group.*

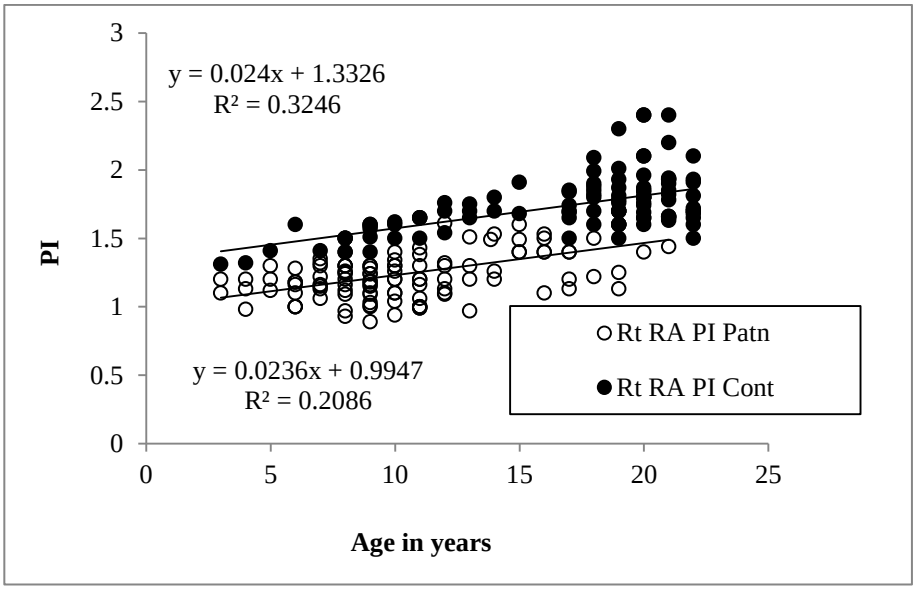

Figure 4.5.*Scatter plot shows the correlation of age in years with Rt renal Artery PI among patient and control group.*

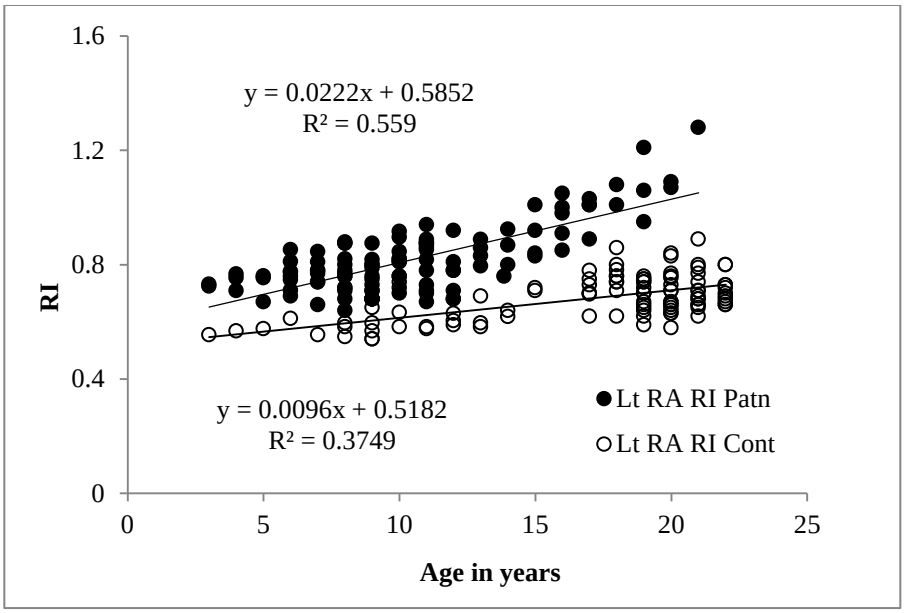

Figure 4.6.*Scatter plot shows the correlation of age in years with Lt renal Artery RI among patient and control group.*

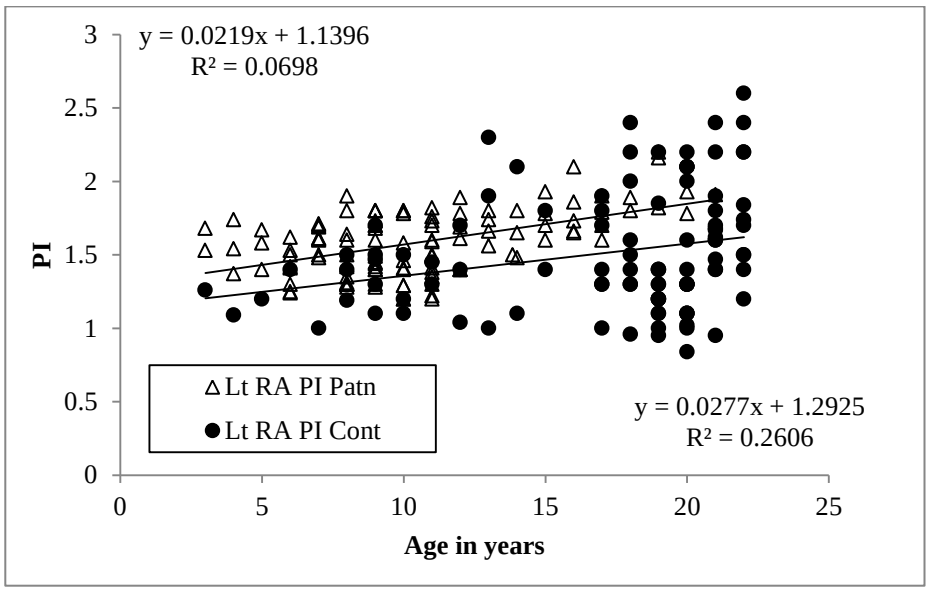

Figure 4.7.*Scatter plot shows the correlation of age in years versus Lt renal Artery PI among patient and control group.*

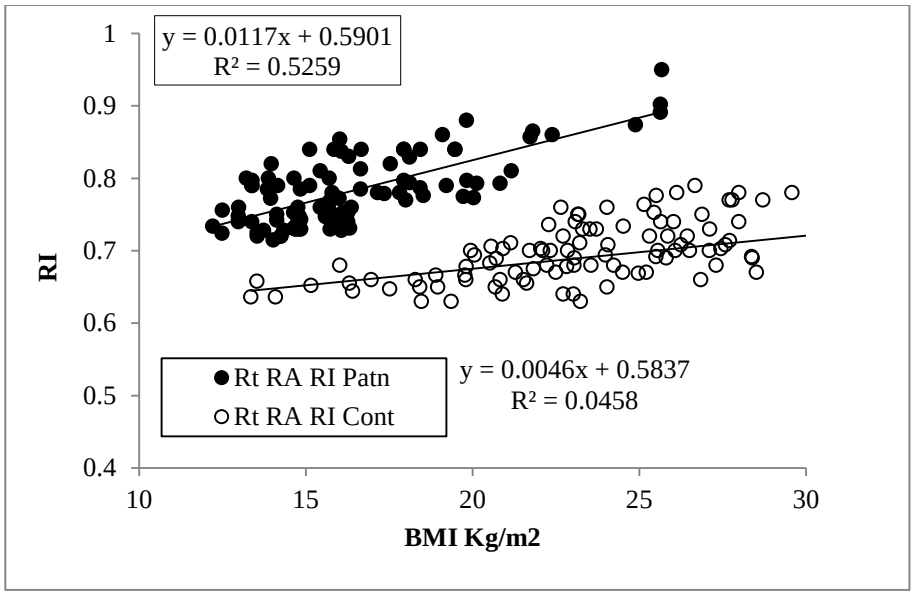

Figure 4.8.*Scatter plot shows the correlation of BMI in Kg/m2 with Rt renal Artery RI among patient and control group.*

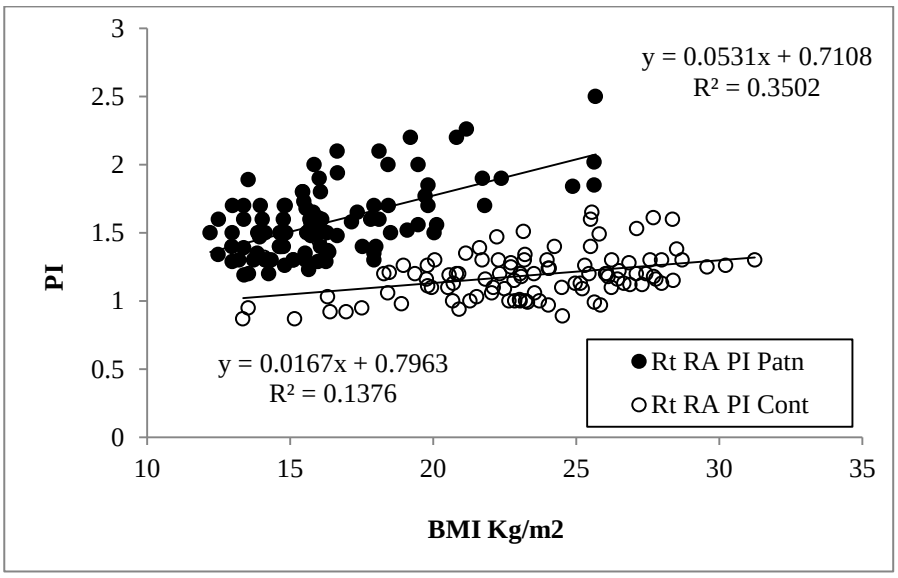

Figure 4.9.*Scatter plot shows the correlation of BMI in Kg/m^2 with Rt renal Artery PI among patient and control group.*

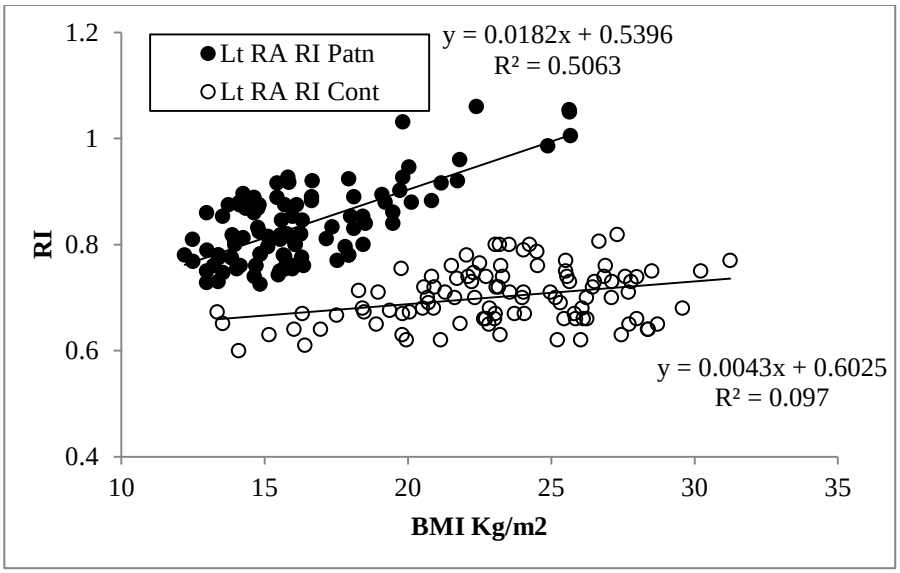

Figure 4.10.*Scatter plot shows the correlation of BMI in Kg/m2 with Lt renal Artery RI among patient and control group.*

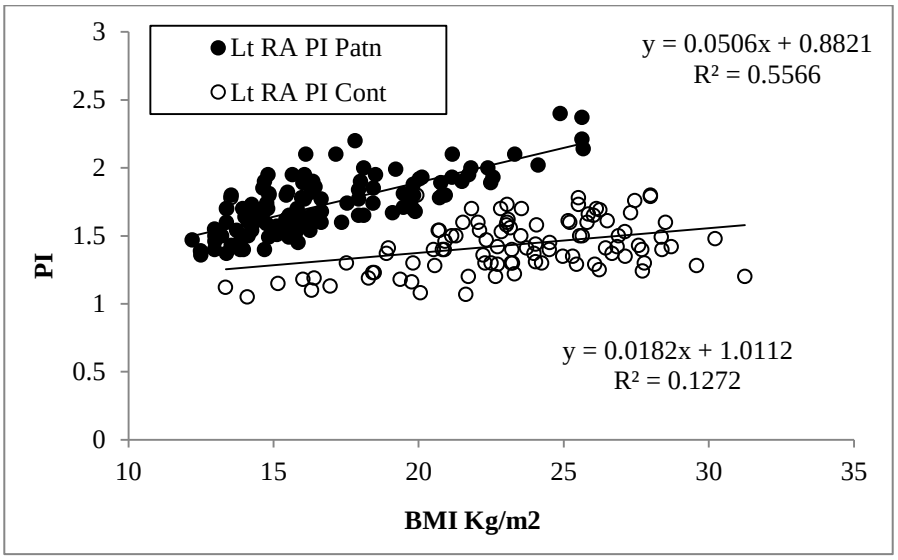

Figure 4.11.*Scatter plot shows the correlation of BMI in Kg/m^2 with Lt renal Artery PI among patient and control group.*

Chapter Five
Discussion, conclusion and recommendations

5. 1 Discussion

This study was conducted to detect early morphological and physiological renal changes in patients with sickle cell disease in Sudan using ultrasonography.

About 115 SCD patients and 100 normal subjects as control group, the study revealed that there were (63) male (54.6%) and 52 female (45.4%) which explain the high incidence of SCD among male (Figure 4.1), no significant justification for this result reported.

The mean age in (years) of SCD patients included in this study was 10.5±4 while 17±4.9 for control group, with their mean BMI (kg/m^2) 16.8±3 & 23.2±5.5 for SCD patients and control group respectively (Table 4.1).

The average measurement of the right kidney length (cm) and volume (cm^3) for SCD patients was 8.78±1.04 & 59.41±2.21 respectively, while the left kidney measures 8.93±5.22/cm (length) & 98.38±21.38/ cm^3 (volume), the control group shows 9.14±1.04/cm and 97.85±29.53/ cm^3 for right kidney length and volume respectively, as well as the left kidney length = 9.5±1.04/cm, while the volume =100.2±22.73/ cm^3 (Table 4.2), so that the left kidney size & volume greater than the right kidney. This result agrees with other researchers Zeb et al (2012) and Mazin et al, (2014). The justification of this, is that spleen is smaller than liver, so the left kidney has more space to grow and it is also found that, the left renal artery is shorter than the right, so increased blood flow in the left renal artery may result in relatively increase in volume. .

The blood flow indices of SCD patients in average was 0.8±0.2 and 1.5±0.4, for RI & PI respectively for right renal artery, the left renal artery measures 0.77±0.1 for RI and 1.6±0.2 for PI. The right renal artery of the healthy subjects

shows 0.7±0.1 & 1.4±0.4 for RI & PI respectively, while the RI & PI of left renal artery measure 0.7±0.1 and 1.5±0.5 respectively (Table 4.3), this increment of RI & PI in SCD patients relative to the control group agree with Guvenc et al, (2005), he explain that due to a reduction of renal blood flow and an increase in renal vascular resistance during painful crisis in SCD patients compared with control group.

The effect of SCD on renal echogenicity had been reported in previous studies. The increased echogenicity involves medullae and cortex and may be diffused or focal. In the current study, the incidence of increased echogenicity was 36.5% (42 patients) & 37.4% (43 patients) for right and left kidney respectively (Table 4.4). This result is agreed with Daneil et al. (1993) who reported increased echogenicity in various types of sickle hemoglobinopathies. Our finding was also consistent with Ali et al. (2008) who reported increased focal and diffused echogenicity in 7.1% and 9.5% of the cases. Marina et al. (2003) reported that increased echogenicity was found in17.6% of patients with sickle-cell syndromes. The etiology of increased echogenicity was unknown; however, glomerulofibrosis, renal papillary necrosis, renal sclerosis, increased concentrations of iron deposits within tubular epithelial cells, focal scarring and interstitial fibrosis in vasa recta system have been suggested as contributing factors (Ali et al, 2008).

The result of this study showed that there is a direct linear relationship between age in years and right & left kidney volume among patient with SCD.; it was found that right & left kidney volume increased by 0.629 cm^3& 0.354 cm^3 respectively (Figure 4.2).

The study showed statistically significant elevation in RI and PI (Rt & Lt kidneys) among SCD patients compared with controls (Figure 4.3). The right renal artery RI & PI were 0.8±0.2 & 1.5±0.4 respectively in patients with linear

increment of 0.005 & 0.023/year respectively for patients (Figure 4.4 &4.5), while the values of (0.7±0.1 & 1.4±0.4) for RI and PI respectively for control group which increased by 0.002 & 0.024/year respectively (Figure 4.4&4.5).

The left renal artery RI & PI showed 0.77±0.2 & 1.6±0.2 respectively in patients and increased by 0.022 & 0.021/year (Figure 4.6 &4.7). The values of (0.7±0.1 & 1.5±0.5) for RI and PI respectively in control group increased by 0.009 & 0.027 annually for RI and PI respectively (Figure 4.8 &4.9). This results agree with studies conducted by Aikimbaev et al, (1996) in which they reported that: there were high renal PIs and RIs in patients with SCD compared with control subjects and as well Taori et al, (2008) reported that both RIs and PIs (in the main renal, segmental, and interlobar arteries) were significantly higher in 62 Indian patients with SCD as compared with normal controls. Such high RI and PI among SCD patients ascribed to the increased renal vascular tone resulting from the various vascular occlusive mechanisms occurring in sickle affected kidneys as justified by Robert et al, (1991).

The result of this study showed that there is a direct proportional linear relationship between RI and BMI for the Rt renal artery in patients and control group; however the increment of patient RI increased by 0.011 kg/m^2 relative to control group which was increased by a factor of 0.004kg/m^2 (Figure 4.8). Similarly the BMI has direct relationship with PI; where it increased by 0.053kg/m^2 & 0.016kg/m^2 (Figure 4.9).

The relation between BMI and RI in the Lt renal artery showed that the RI values increased by 0.018/kg/m^2 in patients and 0.004/kg/m2 in control group (Figure 4.10). Also the PI has direct proportional relationship with BMI in the Lt renal artery in patients and healthy one, PI was increased by 0.050/kg/m2& 0.018/kg/m2 in patients and control group respectively (Figure 4.11).

5.3 Conclusion

After the scoring of the thesis objectives, the worth points to be implied in the conclusion would be as follows:

The incidence of SCD among the selected sample was greater in male than female and the most of patients were children.

The right and left kidney in SCD patients were atrophied relative to control group.

The RIs and PIs for the right and left renal arteries of patients were greater than in control group, and as well the SCD used to increase the echogenicity of the kidneys.

The study also revealed that: there is a direct proportional linear relationship between RI and BMI for the right renal artery in patients and control group; with prominent increment for patient RI relative to control group. Similarly the PI increases with BMI in SCD patients more than control group.

Also the left renal artery RIs & PIs has direct proportional linear relationship with BMI in SCD patients and control group.

Since the sickle cell disease has an impact in kidneys, the worth outcome of this study proved that: Kidneys ultrasonography as kidneys volume, echogenicity and renal artery RIs & PIs could be used successfully as early sonographic predictors of kidneys changes for SCD and/or other diseases which could have same or similar impact in the kidneys at early stage.

5.4 Recommendations

The worth recommended points after successful finishing of the thesis could summarize in the following points:

- Further studies could conduct in the same region to reveal the hereditary diseases and their consequences in human health and progeny.
- Regular ultrasound scanning for kidneys is recommended for SCD patients to detect renal changes.
- Encouraging the population for marriage from non relative ones.
- Establishing more specialized centers with modern equipment.
- Community education and awareness about the morbidities of the SCD.
- Writing scientific papers in SCD that implies more parameters to verify it is relationship with tribal factor, race and genes.
- Study of organs related to the kidneys such as adrenal glands
- Using other modalities like computed tomography adjuvant to ultrasonography.

References

Abdullah. B, Garelnabi, M. E. M., Ayad, C. E., & Ahmed, E. (2014). Establishment of Reference Values for Renal Length and Volume for Normal Adult Sudanese using M RI Disc Summation Method. *Global Journal of Medical Research*, *14*(2).

Adeela Arooj, Jostinah Lam, Yeoh J.Wui, Eko Supriyanto. (2011). Comparison of Renal Size among Different Ethnicities, International Journal Of Biology And Biomedical Engineering, Volume 5, Issue 4: 221- 229.

Adeva, M., El-Youssef, M., Rossetti, S., Kamath, P. S., Kubly, V., Consugar, M. B., & Harris, P. C. (2006). Clinical and molecular characterization defines a broadened spectrum of autosomal recessive polycystic kidney disease (ARPKD). *Medicine*, *85*(1), 1-21.

Aikimbaev KS1, Oğuz M, Güvenç B, Başlamişli F, Koçak R. (1996). Spectral pulsed Doppler sonography of renal vascular resistance in sickle cell disease: clinical implications. Br. J. Radiol. 69(828), 1125-1129. DOI: 10.1259/0007-1285-69-828-1125.

Ali Balcı, Sinem Karazincir, Özlem Sangün, Edip Gali, & Turgay Daplan. (2008) Prevalence of abdominal ultrasonographic abnormalities in patients with sickle cell disease. Diagn Interv Radiol 14(3): 136-137.

Attalla, B. I. (2010). Abdominal sonographic findings in children with sickle cell anemia. Journal of Diagnostic Medical Sonography, 26(6), 281-285.)

Avasthi PS, Voyles WF, Greene ER. (1984). Noninvasive diagnosis of renal artery stenosis by echo-Doppler velocimetry. Kidney Int. 25, 824-829.

Balci, A., Karazincir, S., Sangün, Ö., Gali, E., Daplan, T., Cingiz, C., & Egilmez, E. (2008). Prevalence of abdominal ultrasonographic abnormalities in patients with sickle cell disease. Diagnostic and Interventional Radiology, 14(3), 133.

Brandt TD, Neiman HL, Dragowski MJ, Bulawa W, Claykamp G. (1982). Ultrasound assessment of normal renal dimensions Journal Ultrasound Med. (2):49-52.

Clarke GM, Higgins TN. (2000). "Laboratory investigation of hemoglobinopathies and thalassemias: review and update". Clin. Chem. 46 (8 Pt 2): 1284-90. PMID 10926923.

Daniel Zinn, Jack O, Harris L (1993) Focal and diffused echogenicity in the renal parenchyma in patients with sickle hemoglobinopathies-an Observational study. Jultrasound Med 12(4): 211-214.

Emamian SA, Nielson MB, Pedersen JF, Ytte L. (1993) Kidney dimensions at sonography: correlation with age, sex, and habitus in 665 adult volunteers. AJR; 160:83-86.

Gerard J. Tortora Bergen & Bryan Derrickson. (2012). Principles of Anatomy & physiology 13th Edition pub: John Wiley & Sons, Inc.

Glassberg J. (2011). "Evidence-based management of sickle cell disease in the emergency department". Emergency Medicine Practice 13 (8): 1-20; quiz 20. PMID 22164362.

Glodny, B., Unterholzner, V., Taferner, B., Hofmann, K. J., Rehder, P., Strasak, A., & Petersen, J. (2009). Normal kidney size and its influencing factors-a 64-slice MDCT study of 1.040 asymptomatic patients. BMC urology, 9(1), 19.

Guvenc, B., Aikimbaev, K., Unsal, C., Akgul, E., Gurkan, E., Binokay, F., & Besena, A. (2005). Renal vascular resistance in sickle cell painful crisis. International journal of hematology, 82(2), 127-131.

Harrow BR, Sloane JA, Liebman NC. (1963). Roentgenologic demonstration of renal papillary necrosis in sickle cell trait. N Engl J Med. 268, 969-976.

Heine GH, Gerhart MK, Ulrich C (2005): Renal Doppler resistance indices are associated with systemic atherosclerosis in kidney transplant recipients. Kidney Int. Aug; 68(2):878-85.

Herrick JB. (2001).Peculiar elongated and sickle-shaped red blood corpuscles in a case of severe anemia. Yale Journal of Biol. Med. 74(3), 179–184.

Hildebrandt F, Benzing T, Katsanis N. Ciliopathies. N. (2011). Engl J Med.; 364 (16):1533–1543.

Ibinaiye, P. O., Babadoko, A. A., Yusuf, R., & Hassan, A. A. (2013). Renal complications of sickle cell anemia in Zaria, Nigeria: An ultrasonographic assessment. West African Journal of Radiology, 20(1), 19.

Kishor B. Taori, Ritu S. Chaudhary, VinodAttarde, Suresh Dhakate, VirenderSheorain, PrashantNimbalkar and Preetam N. Wasnik. (2008). Renal Doppler Indices in Sickle Cell Disease: Early Radiologic Predictors of Renovascular Changes. American Journal of Roentgenology, vol. 191(1), 239-242. DOI:10.2214/AJR.07.3125.

Lee, C., Davies, S., & Dezatoux, C. (2000). Neonatal Screening for sickle cell disease. The Cochrane Collaboration. John Wiley & Sons, Ltd.

Lin ZY, Wang LY, Yu ML, Dai CY, Chen SC, Chuang WL, Hsieh MY, Tsai JF, Chang WY. (2002) Influence of age on intrarenal resistive index measurement in normal .subjects. Abdom Imaging; 28: 230-2.

Marina G Papadaki, Antonios C Kattamis, Irene G. (2003) Pediatric Radiology 33(8): 515-521.

Moghazi, S., Jones, E., Schroepple, J., Arya, K., Mcclellan, W., Hennigar, R. A., & O'Neill, W. C. (2005). Correlation of renal histopathology with sonographic findings. Kidney international, 67(4), 1515-1520.

Mostbeck, G. H., Kain, R., Mallek, R., Derfler, K., Walter, R., Havelec, L., & Tscholakoff, D. (1991). Duplex Doppler sonography in renal parenchymal disease. Histopathologic correlation. Journal of ultrasound in medicine, 10(4), 189-194.

Mujahid Raza, Amina Hameed, M Imran Khan. (2011) Ultrasonographic Assessment of Renal Size and Its Correlation with Body Mass Index in Adults without Known Renal Disease,J Ayub Med Coll Abbottabad;23(3): 64-68.

Nath, K. A., & Hebbel, R. P. (2015). Sickle cell disease: renal manifestations and mechanisms. Nature reviews Nephrology, 11(3), 161-171.

Ohta, Y., Fujii, K., Arima, H., Matsumura, K., Tsuchihashi, T., Tokumoto, M., & Iida, M. (2005). Increased renal resistive index in atherosclerosis and diabetic nephropathy assessed by Doppler sonography. Journal of hypertension, 23(10), 1905-1911.

Olujohungbe A, Burnett AL. (2013). "How I manage priapism due to sickle cell disease". British Journal of Haematology 160 (6): 754-65. doi:10.1111/bjh.12199. PMID 23293942.

Papadaki, M. G., Kattamis, A. C., Papadaki, I. G., Menegas, D. G., Georgakopoulou, T. P., Mavrommati-Metaxotou, A., & Kattamis, C. A. (2003). Abdominal ultrasonographic findings in patients with sickle-cell anaemia and thalassaemia intermedia. Pediatric radiology, 33(8), 515-521.

Pham PT, Pham PC, Wilkinson AH, Lew SQ. (2000). Renal abnormalities in sickle cell disease. Kidney Int., 57, 1–8.

Powars D, Chan L, Schroeder W. (1990). The variable expression of sickle cell disease is genetically determined. Semin Hematol. 27, 360-376.

Radermacher, J., Ellis, S., & Haller, H. (2002). Renal resistance index and progression of renal disease. Hypertension, 39(2), 699-703.

Radermacher, J. (2005). Ultrasonography of the kidney and the renal vessels. Part I: Normal findings, inherited and renoparenchymatous diseases. UROLOGE, 44(11), 1351-1363.

Robert B. Francis, Jr, and Cage S. Johnson. (1991). Vascular Occlusion in Sickle Cell Disease: Current Concepts and Unanswered Questions. The Journal of the American Society of Hematology, 77(7), 1405-1414.

Rodgers PM, Bates JA, Irving HC. (1992). Intrarenal doppler ultrasound studies in normal and acutely obstructed kidneys. Br. J.Radiol. 65, 207-212.

Rosado, E., Paixão, P., Schmitt, W., Penha, D., Carvalho, F. M. P. D., & Tavares, A. (2014). Sickle cell anemia: a review of the imaging findings. In European Congress of Radiology. European Society of Radiology.

Saeed, Z., Mirza, W., Sayani, R., Sheikh, A., Yazdani, I., & Hussain, S. A. (2012). Sonographic measurement of renal dimensions in adults and its correlates. International Journal of Collaborative Research on Internal Medicine & Public Health.

Schmidt, Günter. (2011) Thieme Clinical Companions: Ultrasound: Ultrasound Thieme.

Shin, H. S., Chung, B. H., Lee, S. E., Kim, W. J., Ha, H. I., & Yang, C. W. (2009). Measurement of kidney volume with multi-detector computed tomography scanning in young Korean. Yonsei medical journal, 50(2), 262-265.

Siddappa, J. K., Singla, S., Al Ameen, M., Rakshith, S. C., & Kumar, N. (2013) Correlation of ultrasonographic parameters with serum creatinine in chronic kidney disease. Journal of clinical imaging science, 3(1), 28.
Sweeney, W. E., & Avner, E. D. (2014). Polycystic kidney disease, autosomal recessive.

Torres VE, Harris PC, Pirson Y. (2007). Autosomal dominant polycystic kidney disease. Lancet.; 369(9569):1287–1301.

Taori, K. B., Chaudhary, R. S., Attarde, V., Dhakate, S., Sheorain, V., Nimbalkar, P., & Wasnik, P. N. (2008). Renal Doppler indices in sickle cell disease: early radiologic predictors of renovascular changes. American Journal of Roentgenology, 191(1), 239-242.

Vasaikar, N. B., Sonawane, S., Patil, S., Borse, L. B., Borse, S. L., & Pawar, S. P. (2015). A review on sickle cell anemia. Pharma Science Monitor, 6(2), 118-132.

Walker TM, Beardsall K, Thomas PW, Serjeant GR. (1996). Renal length in sickle cell disease: observations from a cohort study. Clin. Nephrol. 46, 384-388.